NACA TN 3368 9655

TECH LIBRARY KAFB, NM
0065928

NATIONAL ADVISORY COMMITTEE FOR AERONAUTICS

TECHNICAL NOTE 3368

ANALYSIS OF BEHAVIOR OF SIMPLY SUPPORTED FLAT PLATES COMPRESSED BEYOND THE BUCKLING LOAD INTO THE PLASTIC RANGE

By J. Mayers and Bernard Budiansky

Langley Aeronautical Laboratory
Langley Field, Va.

Washington
February 1955

AFMDC
TECHNICAL LIBRARY
AFL 2811

1Q

TECH LIBRARY KAFB, NM

0065928

NATIONAL ADVISORY COMMITTEE FOR AERONAUTIC.

TECHNICAL NOTE 3368

ANALYSIS OF BEHAVIOR OF SIMPLY SUPPORTED FLAT PLATES COMPRESSED BEYOND THE BUCKLING LOAD INTO THE PLASTIC RANGE

By J. Mayers and Bernard Budiansky

SUMMARY

An analysis is presented of the postbuckling behavior of a simply supported, square flat plate with straight edges compressed beyond the buckling load into the plastic range. The method of analysis involves the application of a variational principle of the deformation theory of plasticity in conjunction with computations carried out on a high-speed calculating machine. Numerical results are obtained for several plate proportions and for one material. The results indicate plate strengths greater than those that have been found experimentally on plates that do not satisfy straight-edge conditions.

INTRODUCTION

The determination of the load-carrying capacity of a plate subjected to loads in its plane depends upon a knowledge of the behavior of the plate in the postbuckled range. Postbuckling analyses of plates have for the most part been based on purely elastic considerations. However, the relatively thick plate elements used in modern aircraft structures may generally be expected to undergo plastic deformations prior to failure of the components that they constitute. Consequently, the theoretical determination of the loads that such plates can support requires the incorporation of plasticity theory into a large-deflection postbuckling analysis.

Many authors have investigated the elastic postbuckling behavior of flat plates in compression; the more widely known of these investigations are references 1 to 11. The basic differential equations for a plate element undergoing large deflections are derived by Von Kármán in reference 1. In reference 2, Von Kármán introduces the concept of the effective width of postbuckled plates. Various approximate solutions for postbuckling behavior are presented in references 3, 4, 5, and 6 by Cox, Timoshenko, Marguerre and Trefftz, and Marguerre,

respectively, where analyses are carried out by energy methods. In reference 7, Kromm and Marguerre obtain very accurate results at moderately exceeded buckling loads for simply supported, infinitely long plates in compression by extending the investigations of references 5 and 6. An essentially exact solution for square plates in compression is presented by Levy in reference 8, where the large-deflection equations of reference 1 are solved to a high degree of approximation by means of Fourier series. In reference 9, Koiter improves the results of reference 7 to make them applicable far beyond buckling; in addition, results are presented for clamped plates. The effects of initial deviations from flatness for square plates are investigated by Hu, Lundquist, and Batdorf in reference 10 and by Coan in reference 11 by means of the method of solution advanced in reference 8. In reference 10, the side edges of the plate are constrained to remain straight, whereas, in reference 11, the side edges are free to distort in the plane of the plate.

The large number of investigations of the elastic postbuckling problem and the fact that solutions can be obtained only by approximate methods indicate to some extent the unwieldiness of the nonlinear, large-deflection equations involved in the postbuckling problem. The lack of solutions to the corresponding inelastic problem appears to be a consequence not only of its large-deflection aspects but also of nonlinearity in the stress-strain relations. The inelastic problem is further complicated by the fact that some question exists as to the appropriate plastic stress-strain law applicable to the states of combined stress involved in the problem.

In recent years, much work has been done in formulating variational principles for theories of plasticity. At the same time, great advances have been made in the development of high-speed computing machines. The use of a variational principle in conjunction with calculations performed on a high-speed computer appears to offer a feasible approach to the solution of the inelastic postbuckling problem. In the present paper, this approach is used to determine the behavior of an aluminum-alloy, simply supported, square flat plate with edges constrained to remain straight, compressed beyond the (elastic) buckling stress into the plastic range. The variational principle used applies to the simple deformation theory of plasticity and the calculations were made on the Standards' Eastern Automatic Computer (SEAC) of the National Bureau of Standards.

The results of the analysis are presented in the form of curves showing the variation of deformations, stress distribution, average compressive stress, and effective width with the applied unit shortening.

SYMBOLS

E	Young's modulus for plate material
E_s	secant modulus
M_x, M_y	bending moments per unit length
M_{xy}	twisting moment per unit length
U	strain energy of plate
V	volume of plate
b	plate dimension in x- and y-direction
b_e	effective width of plate
e	unit shortening applied to plate
e_{cr}	compressive buckling strain or shortening
f	unit displacement of plate side edges
h	overall thickness of two-element plate measured between center lines of faces
i, m, n, p, q	integers
t	thickness of homogeneous or solid plate
t_f	thickness of face of two-element plate
u, v, w	displacement of point on middle surface of plate in x-, y-, and z-direction, respectively
x, y, z	plate coordinates (see fig. 1)
γ_{xy}'	middle-surface shear strain
γ_{xy}''	twisting strain
γ_{xy}	total shear strain in xy-plane

ϵ_{eff}	effective strain, $\frac{2}{\sqrt{3}}\sqrt{\epsilon_x^2 + \epsilon_y^2 + \epsilon_x\epsilon_y + \frac{\gamma_{xy}^2}{4}}$
ϵ_x', ϵ_y'	middle-surface strains in x- and y-direction, respectively
ϵ_x'', ϵ_y''	bending strains in x- and y-direction, respectively
ϵ_x, ϵ_y	total components of strain in x- and y-direction, respectively
ξ	nondimensional lateral coordinate, $2x/b$
η	nondimensional axial coordinate, $2y/b$
μ	Poisson's ratio for plate material
σ_{av}	average compressive stress
σ_{cy}	compressive yield stress of material
σ_{cr}	compressive buckling stress
σ_{eff}	effective stress, $\sqrt{\sigma_x^2 + \sigma_y^2 - \sigma_x\sigma_y + 3\tau_{xy}^2}$
σ_x, σ_y	components of stress in x- and y-direction, respectively
$\bar{\sigma}_x$, $\bar{\sigma}_y$	local average axial and lateral stresses
$\bar{\tau}_{xy}$	local average shear stress
τ_{xy}	shear stress in xy-plane

Subscripts:

t	top face of two-element plate
b	bottom face of two-element plate

THEORY

Statement of the Problem and Basic Assumptions

The problem under consideration is to determine the behavior of a square flat plate compressed unidirectionally beyond the elastic buckling stress into the range where plastic yielding of the material takes place. All edges of the plate are assumed to remain in the original plane of the plate and to have vanishing bending moments. The plate is considered to be subjected to a uniform shortening by means of a pair of rigid, frictionless loading platens; thus, the loaded edges remain straight and free of tangential stresses. The side edges - those parallel to the direction of loading - are assumed to be held straight but are free to translate laterally and are devoid of tangential stresses. The plate is further assumed (fig. 1) to consist of two stress-carrying faces only, the stresses being constant through the thickness of each face. The effects of finite transverse shear stiffness, however, are neglected.

The choice of aspect ratio and edge conditions for the plate is based upon the observed behavior of an interior bay of a multiple-bay stiffened panel immediately after buckling. In general, nearly square buckles form in the skin, and the number of buckles in the longitudinal direction tends to persist in the postbuckling range; thus, the buckles tend to remain nearly square. The behavior is somewhat different in the case of the truly infinitely long plates analyzed in references 7 and 9 where it is shown that the buckles tend to shorten in the direction of loading as the load is increased. The restriction to square buckles made in the present paper is therefore considered to apply to panels that are long enough for nearly square buckles to be formed but not so long that the number of buckles can readily change.

The two-element configuration assumed for the plate is incorporated into the problem in order to simplify the analysis by making it independent of the effects of plasticity through the thickness of the plate.

The question of what is the correct relation between stresses and strains under combined stresses in the plastic region is at present quite unsettled. The literature contains analyses of plastic buckling (see refs. 12 and 13) that have been carried out, with evident success, on the basis of the simple secant-modulus deformation theory of plasticity. On the other hand, serious doubts exist concerning the legitimacy of applying this theory when, as in buckling, the stresses may deviate sharply from so-called "proportional loading" - loading in which the components of stress at any point remain proportional to one another. A considerable controversy on this subject which will not be delved into in this paper has arisen. The course followed in this report is to use deformation theory but to consider plates that buckle <u>elastically</u>. In

such cases, where the postbuckled configuration has had an opportunity to begin to develop elastically, the stress history in the plastic range would not involve widespread, sudden deviations from proportional loading; consequently, simple deformation theory may be used with some degree of confidence.

In the present paper, Poisson's ratio is assumed to be equal to 1/2 in both the elastic and plastic domains; hence, material compressibility is neglected. According to the secant-modulus theory for an incompressible material, the relationship between the instantaneous states of stress and strain at any point in the plate is given by

$$\left.\begin{aligned} \sigma_x &= \frac{4}{3} E_s\left(\epsilon_x + \frac{1}{2}\epsilon_y\right) \\ \sigma_y &= \frac{4}{3} E_s\left(\epsilon_y + \frac{1}{2}\epsilon_x\right) \\ \tau_{xy} &= \frac{1}{3} E_s \gamma_{xy} \end{aligned}\right\} \tag{1a}$$

or

$$\left.\begin{aligned} \epsilon_x &= \frac{1}{E_s}\left(\sigma_x - \frac{1}{2}\sigma_y\right) \\ \epsilon_y &= \frac{1}{E_s}\left(\sigma_y - \frac{1}{2}\sigma_x\right) \\ \gamma_{xy} &= \frac{3}{E_s}\tau_{xy} \end{aligned}\right\} \tag{1b}$$

The quantity E_s is defined by the relationship

$$E_s = \frac{\sigma_{eff}}{\epsilon_{eff}} \tag{2}$$

where σ_{eff} is an effective local stress given by

$$\sigma_{eff} = \sqrt{\sigma_x^2 + \sigma_y^2 - \sigma_x\sigma_y + 3\tau_{xy}^2} \tag{3}$$

and ϵ_{eff} is an effective local strain given by

$$\epsilon_{eff} = \frac{2}{\sqrt{3}}\sqrt{\epsilon_x^2 + \epsilon_y^2 + \epsilon_x\epsilon_y + \frac{\gamma_{xy}^2}{4}} \tag{4}$$

The effective stress and strain are related by the uniaxial stress-strain curve of the material. Thus, E_s can be determined by entering the uniaxial stress-strain curve with either σ_{eff} or ϵ_{eff}.

Equations (1) are strictly applicable at any point in the plate only if the effective stress and strain at that point have never decreased while in the plastic range. The use of equations (1) for any stress history corresponds to a nonlinear elastic material whose uniaxial loading and unloading stress-strain curves are identical. The present solution will be actually carried out for this hypothetical material by assuming equation (1) to apply always, and the applicability to the plastic material will then be assessed a posteriori by examining whether the effective strain does indeed increase monotonically once it enters the nonlinear range.

Basic Equations

In the present paper, the displacements u, v, and w of the middle surface (see fig. 1) will be considered as the basic unknowns to be sought. Since, after buckling, the displacement w can no longer be considered small in comparison with the plate thickness, the postbuckling problem requires application of finite-deflection theory to describe the relationships between strains and displacements.

From reference 4, the expressions relating middle-surface strains and displacements are

$$\left.\begin{aligned} \epsilon_x' &= \frac{\partial u}{\partial x} + \frac{1}{2}\left(\frac{\partial w}{\partial x}\right)^2 \\ \epsilon_y' &= \frac{\partial v}{\partial y} + \frac{1}{2}\left(\frac{\partial w}{\partial y}\right)^2 \\ \gamma_{xy}' &= \frac{\partial u}{\partial y} + \frac{\partial v}{\partial x} + \frac{\partial w}{\partial x}\frac{\partial w}{\partial y} \end{aligned}\right\} \tag{5a}$$

The bending and twisting strains acting throughout the thickness of a plate element are obtained from reference 4 as

$$\left.\begin{aligned} \epsilon_x'' &= z\frac{\partial^2 w}{\partial x^2} \\ \epsilon_y'' &= z\frac{\partial^2 w}{\partial y^2} \\ \gamma_{xy}'' &= 2z\frac{\partial^2 w}{\partial x\,\partial y} \end{aligned}\right\} \tag{5b}$$

where z, in general, is the distance from the middle surface. In the case of the two-element plate, z is taken to be $\pm\frac{h}{2}$, the distances from the middle surface to the median surfaces of the faces.

With the use of the subscripts t and b to denote the top and bottom faces, respectively, the face strains can now be written as

$$\left.\begin{aligned}
\epsilon_{x_{t,b}} &= \frac{\partial u}{\partial x} + \frac{1}{2}\left(\frac{\partial w}{\partial x}\right)^2 \pm \frac{h}{2}\frac{\partial^2 w}{\partial x^2} \\
\epsilon_{y_{t,b}} &= \frac{\partial v}{\partial y} + \frac{1}{2}\left(\frac{\partial w}{\partial y}\right)^2 \pm \frac{h}{2}\frac{\partial^2 w}{\partial y^2} \\
\gamma_{xy_{t,b}} &= \frac{\partial u}{\partial y} + \frac{\partial v}{\partial x} + \frac{\partial w}{\partial x}\frac{\partial w}{\partial y} \pm h\frac{\partial^2 w}{\partial x\,\partial y}
\end{aligned}\right\} \tag{6}$$

The stress-strain relations (eqs. (1a)), in conjunction with the strain-displacement relations (eqs. (6)), give the stresses in the top and bottom faces as

$$\left.\begin{aligned}
\sigma_{x_{t,b}} &= \frac{4}{3}E_{s_{t,b}}\left\{\frac{\partial u}{\partial x} + \frac{1}{2}\frac{\partial v}{\partial y} + \frac{1}{2}\left[\left(\frac{\partial w}{\partial x}\right)^2 + \frac{1}{2}\left(\frac{\partial w}{\partial y}\right)^2\right] \pm \frac{h}{2}\left(\frac{\partial^2 w}{\partial x^2} + \frac{1}{2}\frac{\partial^2 w}{\partial y^2}\right)\right\} \\
\sigma_{y_{t,b}} &= \frac{4}{3}E_{s_{t,b}}\left\{\frac{\partial v}{\partial y} + \frac{1}{2}\frac{\partial u}{\partial x} + \frac{1}{2}\left[\left(\frac{\partial w}{\partial y}\right)^2 + \frac{1}{2}\left(\frac{\partial w}{\partial x}\right)^2\right] \pm \frac{h}{2}\left(\frac{\partial^2 w}{\partial y^2} + \frac{1}{2}\frac{\partial^2 w}{\partial x^2}\right)\right\} \\
\tau_{xy_{t,b}} &= \frac{1}{3}E_{s_{t,b}}\left(\frac{\partial u}{\partial y} + \frac{\partial v}{\partial x} + \frac{\partial w}{\partial x}\frac{\partial w}{\partial y} \pm h\frac{\partial^2 w}{\partial x\,\partial y}\right)
\end{aligned}\right\} \tag{7}$$

Here E_{s_t} and E_{s_b} are considered to be functions of

$$\epsilon_{eff_t} = \frac{2}{\sqrt{3}}\sqrt{\epsilon_{x_t}^{\,2} + \epsilon_{y_t}^{\,2} + \epsilon_{x_t}\epsilon_{y_t} + \frac{\gamma_{xy_t}^{\,2}}{4}} \tag{8a}$$

and

$$\epsilon_{eff_b} = \frac{2}{\sqrt{3}}\sqrt{\epsilon_{x_b}^{\,2} + \epsilon_{y_b}^{\,2} + \epsilon_{x_b}\epsilon_{y_b} + \frac{\gamma_{xy_b}^{\,2}}{4}} \tag{8b}$$

respectively.

The local bending moments produced in the plate by the face stresses are simply

$$\left.\begin{aligned} M_x &= -\left(\sigma_{x_t} - \sigma_{x_b}\right)\frac{h}{2}\,t_f \\ M_y &= -\left(\sigma_{y_t} - \sigma_{y_b}\right)\frac{h}{2}\,t_f \\ M_{xy} &= \left(\tau_{xy_t} - \tau_{xy_b}\right)\frac{h}{2}\,t_f \end{aligned}\right\} \tag{9}$$

and the average stresses at any point in the plate are

$$\left.\begin{aligned} \bar{\sigma}_x &= \frac{1}{2}\left(\sigma_{x_t} + \sigma_{x_b}\right) \\ \bar{\sigma}_y &= \frac{1}{2}\left(\sigma_{y_t} + \sigma_{y_b}\right) \\ \bar{\tau}_{xy} &= \frac{1}{2}\left(\tau_{xy_t} + \tau_{xy_b}\right) \end{aligned}\right\} \tag{10}$$

The conditions of equilibrium in the x-, y-, and z-direction yield (see ref. 4)

$$\frac{\partial \bar{\sigma}_x}{\partial x} + \frac{\partial \bar{\tau}_{xy}}{\partial y} = 0 \tag{11a}$$

$$\frac{\partial \bar{\sigma}_y}{\partial y} + \frac{\partial \bar{\tau}_{xy}}{\partial x} = 0 \tag{11b}$$

$$\frac{\partial^2 M_x}{\partial x^2} - 2\,\frac{\partial^2 M_{xy}}{\partial x\,\partial y} + \frac{\partial^2 M_y}{\partial y^2} = -2t_f\left(\bar{\sigma}_x\,\frac{\partial^2 w}{\partial x^2} + \bar{\sigma}_y\,\frac{\partial^2 w}{\partial y^2} + 2\bar{\tau}_{xy}\,\frac{\partial^2 w}{\partial x\,\partial y}\right) \tag{11c}$$

where $2t_f$, the stress-carrying thickness of the two-element plate, is used in place of the thickness t of the homogeneous plate considered in reference 4.

The boundary conditions stipulated for the present problem are as follows: The prescribed unit shortening e requires that

$$u\left(\pm\frac{b}{2}, y\right) = \mp e\frac{b}{2} \tag{12}$$

The condition that the side edges remain straight is

$$v\left(x,\pm\frac{b}{2}\right) = \text{Constant} \tag{13}$$

The requirement that the side edges be free to translate is

$$\int_{-b/2}^{b/2} \bar{\sigma}_y\left(x,\pm\frac{b}{2}\right)dx = 0 \tag{14}$$

The condition that the tangential stresses vanish on each face is written

$$\bar{\tau}_{xy}\left(\pm\frac{b}{2},y\right) = \bar{\tau}_{xy}\left(x,\pm\frac{b}{2}\right) = 0 \tag{15}$$

Finally, the simple-support conditions stipulate that

$$w\left(\pm\frac{b}{2},y\right) = w\left(x,\pm\frac{b}{2}\right) = 0 \tag{16}$$

and

$$M_x\left(\pm\frac{b}{2},y\right) = M_y\left(x,\pm\frac{b}{2}\right) = 0 \tag{17}$$

Now, the differential equations (11), together with the boundary conditions (eqs. (12) to (17)), may be considered to constitute the complete statement of the problem in terms of the displacements u, v, and w. That is, through the use of equations (6) to (11) and by specification of the uniaxial stress-strain curve, the differential equations (11) could, in principle, be reduced to a set of three differential equations in u, v, and w. Similarly, the boundary conditions depend, implicitly, only on the displacements. An alternative formulation of the problem, less natural but more attractive, is presented in the next section by means of a variational principle.

Variational Principle

The strain energy of stretching and bending for the two-element plate is

$$U = t_f \int_{-b/2}^{b/2} \int_{-b/2}^{b/2} \left(\int_0^{\epsilon_{x_t}} \sigma_{x_t} \, d\epsilon_{x_t} + \int_0^{\epsilon_{y_t}} \sigma_{y_t} \, d\epsilon_{y_t} + \int_0^{\gamma_{xy_t}} \tau_{xy_t} \, d\gamma_{xy_t} \right) dx \, dy + t_f \int_{-b/2}^{b/2} \int_{-b/2}^{b/2} \left(\int_0^{\epsilon_{x_b}} \sigma_{x_b} \, d\epsilon_{x_b} + \int_0^{\epsilon_{y_b}} \sigma_{y_b} \, d\epsilon_{y_b} + \int_0^{\gamma_{xy_b}} \tau_{xy_b} \, d\gamma_{xy_b} \right) dx \, dy \tag{18}$$

It can be readily verified from equations (1) to (4) that

$$\sigma_x \, d\epsilon_x + \sigma_y \, d\epsilon_y + \tau_{xy} \, d\gamma_{xy} = \sigma_{eff} \, d\epsilon_{eff} \tag{19}$$

Thus, the strain-energy expression may be written

$$U = t_f \int_{-b/2}^{b/2} \int_{-b/2}^{b/2} \left(\int_0^{\epsilon_{eff_t}} \sigma_{eff_t} \, d\epsilon_{eff_t} + \int_0^{\epsilon_{eff_b}} \sigma_{eff_b} \, d\epsilon_{eff_b} \right) dx \, dy \tag{20}$$

As a result, in each face of the plate, the strain-energy density at a given point is simply the area under the uniaxial stress-strain curve up to the effective strain level at the point. According to the principle of minimum potential energy for deformation theories (ref. 14), a solution of the present problem renders the strain energy U a relative minimum. Stated precisely, $\delta U = 0$ with respect to <u>admissible</u> variations in u, v, and w. By admissible variations are meant variations that do not violate the <u>geometrical</u> boundary conditions of the problem; in the present problem, the geometrical boundary conditions are given by equations (12), (13), and (16). It is important to note that the variations in displacements need not satisfy the remaining so-called <u>natural</u> boundary conditions (eqs. (14), (15), and (17)).

Although the minimum-potential-energy principle of reference 14 is formulated for small-deflection theory, its use in the present problem is valid. It is shown in appendix A, by means of the calculus of variations, that minimization of the strain energy U with respect to admissible variations in displacements leads to satisfaction of the correct differential equations of equilibrium and the natural boundary conditions.

Method of Solution

The solution of the present problem is found approximately by using the Rayleigh-Ritz procedure in conjunction with the variational principle discussed in the preceding section. Expressions for the unknowns u, v, and w are assumed to be in the following form:

$$w = b \sum_{m=1,3\ldots}^{\infty} \sum_{n=1,3\ldots}^{\infty} w_{mn} \cos \frac{m\pi x}{b} \cos \frac{n\pi y}{b} \tag{21}$$

$$u = -ex + b \sum_{p=1}^{\infty} \sum_{q=0}^{\infty} u_{pq} \sin \frac{2p\pi x}{b} \cos \frac{2q\pi y}{b} \tag{22}$$

$$v = fy + b \sum_{p=0}^{\infty} \sum_{q=1}^{\infty} v_{pq} \cos \frac{2p\pi x}{b} \sin \frac{2q\pi y}{b} \tag{23}$$

These expressions satisfy all the geometrical boundary conditions of equations (12), (13), and (16); e is the magnitude of the prescribed unit shortening and the unknown coefficients w_{mn}, u_{pq}, and v_{pq} remain to be determined from the variational principle. In practice, the solution was limited to the determination of only the six unknown coefficients w_{11}, u_{10}, u_{11}, f, v_{01}, and v_{11}.

In the special case of elastic behavior, where σ_{eff} is a linear function of ϵ_{eff} and $E_s = E$ everywhere in the plate, a solution for these coefficients by analytical minimization of equation (20) is feasible and is given in appendix B. In the plastic solution, however, it is necessary to introduce an appropriate uniaxial stress-strain curve in order to evaluate equation (20) and effect its minimization with respect to the six unknown coefficients. Such a minimization by analytical methods appears to be of prohibitive difficulty. Consequently, the course followed was to utilize a high-speed computing machine (SEAC) to carry out the required minimization process numerically. Essentially, the procedure required repeated numerical evaluation of the strain-energy integral (eq. (20)) for systematically varied sets of the unknown coefficients. An exposition of the computational scheme is contained in appendix C.

RESULTS AND DISCUSSION

The compressive stress-strain curve shown in figure 2, typical of 24S-T aluminum alloy, was used as the basic relationship between

σ_{eff} and ϵ_{eff} in the present investigation. The postbuckling analysis was carried out for four different plate proportions, so chosen that the corresponding values of buckling stress were as indicated on figure 2; each plate was taken to have its initial buckling stress in the elastic range.

As shown in appendix B, the elastic buckling stress for the two-element plate is given by

$$\sigma_{cr} = \frac{4}{3} E\left(\frac{\pi h}{b}\right)^2$$

when Poisson's ratio equals 1/2, and the critical unit shortening is

$$e_{cr} = \frac{4}{3}\left(\frac{\pi h}{b}\right)^2$$

The postbuckling state for each plate depends only on e/e_{cr}, the ratio of the applied unit shortening to the critical strain. The final results for loads carried by two-element plates, with Poisson's ratio equal to 1/2, are considered to apply approximately to solid plates having the same values of σ_{cr} and e/e_{cr}. The proportions of the equivalent solid plates are determined by the usual formula:

$$\sigma_{cr} = \frac{E}{3(1 - \mu^2)}\left(\frac{\pi t}{b}\right)^2$$

Displacements and Stresses

By means of the numerical minimization process described in appendix C, approximations to the true values of the unknown coefficients w_{11}, u_{10}, u_{11}, f, v_{01}, and v_{11} in the expressions (21) to (23) for the displacements w, u, and v were determined for each of the four plate proportions considered and for various values of the applied unit shortening ratio e/e_{cr}. For a given unit shortening, the minimization process involved calculation of the strain-energy expression (20) for systematically varied sets of the displacement coefficients, so chosen as to cause the energy to decrease in magnitude continually. For a given unit shortening, estimates of the true displacement coefficients are then provided by those values that yield the lowest energy value found. With the use of numerical minimization, the accuracy of such estimates is limited by the fact that, in the neighborhood of its minimum, the energy is relatively insensitive to changes in the displacement coefficients. Nevertheless, a reasonably consistent

variation of the final coefficients with e/e_{cr} was found and is shown by the faired curves of figures 3 and 4 for the two extreme plate geometries, plates 1 and 4, respectively. Also shown in these figures, for comparison, are the coefficients given by the elastic solution of appendix B, which considers the same number of unknown coefficients. These elastic coefficients constituted the initial values used in the iterative process for minimizing the energy in the plastic range. As can be seen from figures 3 and 4, the largest differences between the elastic and plastic displacements occur for the in-plane displacements u and v; the deflection coefficient w_{11} is very nearly the same for both the elastic and plastic cases.

From the values of displacements, stresses can be found by use of equations (7). The lateral distribution of axial stress $\bar{\sigma}_x$, as determined by equation (10), is shown in figure 5(a) for three different cross sections of plate 1 at a value of e/e_{cr} of 3; similar distributions for plate 4, at a value of e/e_{cr} of 6, are also shown in figure 5(b). These results for the two plates actually correspond to the same unit shortening, since $(e_{cr})_4 = \frac{1}{2}(e_{cr})_1$. Figures 5(c) and 5(d) show the distributions of average lateral stress $\bar{\sigma}_y$ at several longitudinal cross sections of each of the two plates. It may be of interest to note that, in contrast to the results of figure 5, the corresponding elastic solution of appendix B yields axial and lateral stress distributions (eqs. (B10)) that are independent of the x- and y-coordinate, respectively.

In the elastic solution, conditions of equilibrium in the x- and y-direction are satisfied exactly at each point of the plate. The extent to which in-plane equilibrium is satisfied by the plastic solution may be measured in a gross sense by checking the closeness of the values of the resultant axial force at various lateral cross sections; also, the lateral stress distributions may be examined to see whether they produce essentially zero resultant lateral force. The results of such equilibrium checks are illustrated in figure 5, where the average stress values are indicated for each cross-section distribution. It is seen that, although the average lateral stress is close to zero in all cases, there remains some discrepancy between the magnitudes of the average axial stress at the various stations. Based on the mean value of average axial stress for the three cross sections in each case, the percentage spread between the largest and smallest values of average axial stress amounts to 4.8 percent for plate 1 and 7.4 percent for plate 4. It may be of interest, however, to compare these discrepancies with those that would be obtained by calculating plastic stresses on the basis of the elastic displacements that were used in the first cycle of iteration in the minimization process. The average axial-stress values

obtained on this basis are indicated in figure 5 by the values enclosed in parentheses. As can be seen, the spread between the largest and smallest values of average axial stress for each of the plates is substantial, 32.4 percent for plate 1 and 29.5 percent for plate 4. Thus, a significant improvement was achieved by the minimization process.

The strain distributions of plates 1 and 4 and their variations with e/e_{cr} were subjected to a detailed examination in order to determine whether plastic unloading ever occurred. It was found that, up to the largest value of e/e_{cr} considered in the present study, no such unloading did in fact occur. That is, the magnitude of the effective strain ϵ_{eff} in each face continually increased with increasing e at all points in the plate where plastic yielding occurred; at some points (for example, the midpoint of the loaded edge) ϵ_{eff} does decrease immediately after buckling but this unloading occurs in the elastic range.

Relation Between Average Applied Stress and Unit Shortening

The load-carrying capacity and the stiffness of a plate after buckling are determined by the relationship between the average compressive stress σ_{av} and the applied unit shortening. The load-carrying capacity of the plate at a given shortening is simply the product of the average compressive stress and the cross-sectional area whereas the stiffness of the plate after buckling is related to the slope of the curve of average stress against unit shortening.

As has been shown, the resultant axial force obtained in the present solution varies somewhat, depending on the location of the cross section. An appropriate unique value of the average applied stress may be most conveniently determined by means of the following energy considerations.

The strain energy (eq. (20)), which was minimized for various values of e/e_{cr}, must equal the total external work. Therefore,

$$U = 2t_f b^2 \int_0^e \sigma_{av}\, de$$

whence

$$\sigma_{av} = \frac{d}{de}\frac{U}{V} \tag{24}$$

where the plate volume is $V = 2t_f b^2$. Since the minimization process described in appendix C yields values of U/EV directly, the use of

relation (24) to determine σ_{av} is quite convenient. (The same relationship was used in the elastic analysis of reference 9.)

Figure 6 shows the variation of U/EV with e/e_{cr} for each of the four plates investigated. The required differentiation of these curves was effected by means of the graphical procedure described in reference 15, and the resultant curves of σ_{av} against e are shown in figure 7 for the four plates. For comparison, the curves determined by the elastic solution of appendix B are shown for each case.

It should be emphasized that these results are certainly approximate by virtue, among other things, of the fact that only a limited number of coefficients were used in the expressions for the displacements. An estimate of the extent of the inaccuracy may be made by comparing the essentially exact relationship between average stress and unit shortening found by Levy for the elastic case with that given by the approximate elastic solution of appendix B, which considers the same number of coefficients as were used in the plastic solution. This comparison is made in figure 8, which shows σ_{av}/σ_{cr} as a function of e/e_{cr} for these two solutions. Thus, it is reasonable to expect that the curves of figure 7 are reliable only up to values of e/e_{cr} of about 4; this limiting value is noted by tick marks on each of the four curves.

A reasonable procedure for correcting the curves of figure 7 would be to reduce them at each value of e/e_{cr} by the corresponding ratio of the two curves of figure 8. This reduction has been made in figure 9; the curves constitute the final estimates of the present paper for the relationship between average compressive stress and unit shortening for the four plates studied.

An interesting feature of the results of figure 9 is that the average compressive stress carried by each plate does not have a maximum value in the range of unit shortening considered. However, the lack of definite mathematical maximums in the average compressive-stress—unit-shortening curves of figure 9 should, perhaps, not be overemphasized in view of the flatness of these curves and the approximate nature of the present solution. More significant is the fact that the curves indicate load-carrying capacities substantially greater than those that have been found experimentally for plates that do not conform to straight-edge boundary conditions. Such test results (unpublished) have been obtained by R. A. Anderson and M. S. Anderson of the Langley laboratory for plates supported laterally in a V-grooved fixture similar to that used in the classical tests by Schuman and Back (ref. 16). Plates supported by V-grooved fixtures are not, of course, constrained to have straight (in-the-plane) side edges after buckling, and, in addition, the V-grooved fixture does not entirely prevent out-of-plane displacements

of the side edges once initial buckling takes place. Needham, in reference 17, gives the test results found by a number of investigators for the maximum strength of compressed square tubes. Again, the plate elements of square tubes do not satisfy the boundary conditions of straight side edges beyond buckling, and, as is remarked by Needham, failure occurs with passage of the buckle pattern through the corners. A comparison between these test results and the results of the present paper can be made by taking from figure 9 a nominal maximum average stress σ_{max} equal to the stress at the large unit shortening of 0.01 (the highest unit shortening for which computations were carried out). Figure 10 shows the relationship between σ_{max}/σ_{cr} and σ_{cr}/σ_{cy} found in this fashion from figure 9 and also gives the corresponding curve determined by test results on a variety of materials, including 24S-T aluminum, for square tubes (ref. 17) and for plates in V-grooved fixtures tested by Anderson and Anderson. (The results for both types of tests fall essentially on a single curve.)

It appears, then, that maintaining straight-edge boundary conditions leads to higher load-carrying capacities, as indicated by the results of the present analysis. This conclusions is bolstered by the experimental results found by Botman in reference 18, which are also shown in figure 10. Botman, continuing the investigations started by Besseling (ref. 19), used a jig that divided a wide plate into three strips by means of a series of opposed knife edges running longitudinally. This type of fixture represents more closely the boundary conditions of the present investigation than do the V-grooved fixtures or the square tubes and, as can be seen from figure 10, leads to higher plate strengths. Of course, the outside edges of the outer bays still do not conform to the straight-edge condition; one may conjecture, then, that still higher strengths would be achieved from tests on plates with additional bays.

Effective Width

The so-called "effective width" of plate can be readily calculated from the curves of figure 9 by means of the relationship

$$\frac{b_e}{b} = \frac{\sigma_{av}}{\sigma_{SS}}$$

where σ_{SS} is the stress obtained from the stress-strain curve for the value of e that yields a given value of σ_{av}. The variation of b_e/b with e/e_{cr} is shown in figure 11 and is compared with the effective width calculated on the basis of Levy's "exact" elastic solution for the square plate. This comparison shows that, at the higher unit shortenings, the effective widths become somewhat greater than those

given by elastic theory. The early dip of the present results below the elastic curve is a consequence of the fact that plastic strains occur in the interior of the plate at unit shortenings that are still in the elastic range.

CONCLUDING REMARKS

A theoretical analysis has been made of the behavior of a simply supported, square flat plate with straight edges compressed beyond the buckling load into the plastic range. Approximate solutions were carried out numerically for one material and for four different plate proportions; the curves for average compressive stress against unit shortening thus obtained were corrected in a rational fashion to account for the limited number of degrees of freedom used in the analysis.

The method of analysis, involving the application of a variational principle in conjunction with a high-speed computing machine, may be applied to plates with different boundary and loading conditions and of different material properties. The number of degrees of freedom assumed in the displacement functions may be increased, subject to the capacity of the computing machine. The chief difficulty that was encountered in the actual numerical solution was the slowness of satisfactory convergence to minimum energy values. The development of improved methods of effecting numerical minimization of nonlinear functions of many variables would be highly desirable for future application of the method of analysis used in this investigation.

Langley Aeronautical Laboratory,
National Advisory Committee for Aeronautics,
Langley Field, Va., November 23, 1954.

APPENDIX A

VERIFICATION OF VARIATIONAL PRINCIPLE

The purpose of this appendix is to show that the variational condition

$$\delta U = 0 \tag{A1}$$

where U is given by equation (20), is valid for finding a solution to the present problem. The variation of U is taken with respect to admissible variations in u, v, and w, that is, those that do not violate the geometrical boundary conditions (12), (13), and (16). It will be shown that the differential equations (11) and the natural boundary conditions (eqs. (14), (15), and (17)) are consequences of equation (A1).

If the strain-energy density

$$\int_0^{\epsilon_{eff}} \sigma_{eff}\, d\epsilon_{eff}$$

is denoted by $F(\epsilon_x,\epsilon_y,\gamma_{xy})$, equation (20) may be written

$$U = t_f \int_{-b/2}^{b/2}\int_{-b/2}^{b/2} (F_t + F_b)\, dx\, dy$$

where the subscripts t and b refer to the top and bottom faces, respectively. Then, the variation of U with respect to u, for example, is

$$\delta_u U = t_f \int_{-b/2}^{b/2}\int_{-b/2}^{b/2} (\delta_u F_t + \delta_u F_b)\, dx\, dy \tag{A2}$$

Similar expressions hold for variations with respect to v and w.

Now,

$$\delta_u F = \frac{\partial F}{\partial \epsilon_x}\delta_u\epsilon_x + \frac{\partial F}{\partial \epsilon_y}\delta_u\epsilon_y + \frac{\partial F}{\partial \gamma_{xy}}\delta_u\gamma_{xy} \tag{A3}$$

and, again, similar expressions hold for $\delta_v F$ and $\delta_w F$. Since $dF = \sigma_{eff}\, d\epsilon_{eff}$, it follows from equation (19) that

$$\left.\begin{aligned} \frac{\partial F}{\partial \epsilon_x} &= \sigma_x \\ \frac{\partial F}{\partial \epsilon_y} &= \sigma_y \\ \frac{\partial F}{\partial \gamma_{xy}} &= \tau_{xy} \end{aligned}\right\} \tag{A4}$$

From the strain-displacement relations (6), it follows that

$$\delta_u \epsilon_x = \delta_u\left(\frac{\partial u}{\partial x}\right) = \frac{\partial}{\partial x}(\delta u)$$

$$\delta_u \epsilon_y = 0$$

$$\delta_u \gamma_{xy} = \delta_u\left(\frac{\partial u}{\partial y}\right) = \frac{\partial}{\partial y}(\delta u)$$

Hence

$$\delta_u U = t_f \int_{-b/2}^{b/2}\int_{-b/2}^{b/2}\left\{\left[\sigma_{x_t}\frac{\partial}{\partial x}(\delta u) + \tau_{xy_t}\frac{\partial}{\partial y}(\delta u)\right] + \left[\sigma_{x_b}\frac{\partial}{\partial x}(\delta u) + \tau_{xy_b}\frac{\partial}{\partial y}(\delta u)\right]\right\} dx\, dy$$

After integration by parts and with the use of expressions (10), the variation becomes

$$\delta_u U = 2t_f\left[\int_{-b/2}^{b/2} \bar{\sigma}_x\, \delta u \Big|_{x=-b/2}^{x=b/2} dy + \int_{-b/2}^{b/2} \bar{\tau}_{xy}\, \delta u \Big|_{y=-b/2}^{y=b/2} dx - \int_{-b/2}^{b/2}\int_{-b/2}^{b/2}\left(\frac{\partial \bar{\sigma}_x}{\partial x} + \frac{\partial \bar{\tau}_{xy}}{\partial y}\right)\delta u\, dx\, dy\right]$$

But, $\delta u = 0$ at $x = \pm\frac{b}{2}$ $\left(\text{since } u = \mp e\frac{b}{2} \text{ at } x = \pm\frac{b}{2}\right)$. On the other hand, δu is arbitrary at $y = \pm\frac{b}{2}$; hence, the condition $\delta_u U = 0$ requires satisfaction of the boundary conditions

$$\bar{\tau}_{xy}\left(x,\pm\frac{b}{2}\right) = 0$$

as well as of the equilibrium equation (11a),

$$\frac{\partial\bar{\sigma}_x}{\partial x} + \frac{\partial\bar{\tau}_{xy}}{\partial y} = 0$$

Similarly, calculation of $\delta_v U$ leads to

$$\delta_v U = 2t_f\left[\int_{-b/2}^{b/2} \bar{\sigma}_y\ \delta v \Bigg|_{y=-b/2}^{y=b/2} dx + \int_{-b/2}^{b/2} \bar{\tau}_{xy}\ \delta v \Bigg|_{x=-b/2}^{x=b/2} dy - \int_{-b/2}^{b/2}\int_{-b/2}^{b/2}\left(\frac{\partial\bar{\sigma}_y}{\partial y} + \frac{\partial\bar{\tau}_{xy}}{\partial x}\right)\delta v\ dx\ dy\right]$$

Hence, setting $\delta_v U$ equal to zero requires satisfaction of equation (11b):

$$\frac{\partial\bar{\sigma}_y}{\partial y} + \frac{\partial\bar{\tau}_{xy}}{\partial x} = 0$$

Also, since δv is arbitrary at $x = \pm\frac{b}{2}$, it follows that

$$\bar{\tau}_{xy}\left(\pm\frac{b}{2},y\right) = 0$$

On the other hand, by virtue of the straight-edge condition (eq. (13)), δv must be constant at $y = \pm\frac{b}{2}$. Hence,

$$\int_{-b/2}^{b/2} \bar{\sigma}_y\left(x,\pm\frac{b}{2}\right) dx = 0$$

since the constant value of δv at each side edge may be arbitrary.

Thus far, it has been shown that the equilibrium equations (11a) and (11b), as well as the natural boundary conditions (14) and (15),

are consequences of condition (A1). It will now be shown that the remaining equilibrium equation (11c) and natural boundary conditions (17) will follow from the condition $\delta_w U = 0$.

From equations (6),

$$\delta_w \epsilon_{x_{t,b}} = \frac{\partial w}{\partial x}\frac{\partial(\delta w)}{\partial x} \pm \frac{h}{2}\frac{\partial^2(\delta w)}{\partial x^2}$$

$$\delta_w \epsilon_{y_{t,b}} = \frac{\partial w}{\partial y}\frac{\partial(\delta w)}{\partial y} \pm \frac{h}{2}\frac{\partial^2(\delta w)}{\partial y^2}$$

$$\delta_w \gamma_{xy_{t,b}} = \frac{\partial w}{\partial x}\frac{\partial(\delta w)}{\partial y} + \frac{\partial w}{\partial y}\frac{\partial(\delta w)}{\partial x} \pm h\frac{\partial^2(\delta w)}{\partial x\,\partial y}$$

Hence,

$$\begin{aligned}\delta_w U = t_f \int_{-b/2}^{b/2}\int_{-b/2}^{b/2} \Bigg\{ &\left(\sigma_{x_t} + \sigma_{x_b}\right)\frac{\partial w}{\partial x}\frac{\partial(\delta w)}{\partial x} + \left(\sigma_{y_t} + \sigma_{y_b}\right)\frac{\partial w}{\partial y}\frac{\partial(\delta w)}{\partial y} + \\ &\left(\tau_{xy_t} + \tau_{xy_b}\right)\left[\frac{\partial w}{\partial x}\frac{\partial(\delta w)}{\partial y} + \frac{\partial w}{\partial y}\frac{\partial(\delta w)}{\partial x}\right] + \left(\sigma_{x_t} - \sigma_{x_b}\right)\frac{h}{2}\frac{\partial^2(\delta w)}{\partial x^2} + \\ &\left(\sigma_{y_t} - \sigma_{y_b}\right)\frac{h}{2}\frac{\partial^2(\delta w)}{\partial y^2} + \left(\tau_{xy_t} - \tau_{xy_b}\right)h\frac{\partial^2(\delta w)}{\partial x\,\partial y}\Bigg\}\,dx\,dy\end{aligned}$$

Through the use of relations (9) and (10) and after integration by parts, the variation becomes

$$\begin{aligned}\delta_w U = &\int_{-b/2}^{b/2}\left(2t_f\bar{\sigma}_x\frac{\partial w}{\partial x} + 2t_f\bar{\tau}_{xy}\frac{\partial w}{\partial y} + \frac{\partial M_x}{\partial x} - \frac{\partial M_{xy}}{\partial y}\right)\delta w\,\Bigg|_{x=-b/2}^{x=b/2}dy + \int_{-b/2}^{b/2}\Bigg(2t_f\bar{\sigma}_y\frac{\partial w}{\partial y} + 2t_f\bar{\tau}_{xy}\frac{\partial w}{\partial x} + \\ &\frac{\partial M_y}{\partial y} - \frac{\partial M_{xy}}{\partial x}\Bigg)\delta w\,\Bigg|_{y=-b/2}^{y=b/2}dx - \int_{-b/2}^{b/2}M_x\delta\frac{\partial w}{\partial x}\,\Bigg|_{x=-b/2}^{x=b/2}dy - \int_{-b/2}^{b/2}M_y\delta\frac{\partial w}{\partial y}\,\Bigg|_{y=-b/2}^{y=b/2}dx + \\ &\int_{-b/2}^{b/2}M_{xy}\delta\frac{\partial w}{\partial y}\,\Bigg|_{x=-b/2}^{x=b/2}dy + \int_{-b/2}^{b/2}M_{xy}\delta\frac{\partial w}{\partial x}\,\Bigg|_{y=-b/2}^{y=b/2}dx - \int_{-b/2}^{b/2}\int_{-b/2}^{b/2}\Bigg(2t_f\bar{\sigma}_x\frac{\partial^2 w}{\partial x^2} + \\ &2t_f\bar{\sigma}_y\frac{\partial^2 w}{\partial y^2} + 4t_f\bar{\tau}_{xy}\frac{\partial^2 w}{\partial x\,\partial y} + \frac{\partial^2 M_x}{\partial x^2} - 2\frac{\partial^2 M_{xy}}{\partial x\,\partial y} + \frac{\partial^2 M_y}{\partial y^2}\Bigg)\delta w\,dx\,dy\end{aligned}$$

Now, if $\delta_w U$ is to vanish for all admissible values of δw, $\delta \frac{\partial w}{\partial x}$, and $\delta \frac{\partial w}{\partial y}$, then it is readily seen that satisfaction of $\delta_w U = 0$ requires that

$$M_x\left(\pm\frac{b}{2},y\right) = M_y\left(x,\pm\frac{b}{2}\right) = 0$$

and

$$\frac{\partial^2 M_x}{\partial x^2} - 2\frac{\partial^2 M_{xy}}{\partial x\,\partial y} + \frac{\partial^2 M_y}{\partial y^2} = -2t_f\left(\bar{\sigma}_x\frac{\partial^2 w}{\partial x^2} + \bar{\sigma}_y\frac{\partial^2 w}{\partial y^2} + 2\bar{\tau}_{xy}\frac{\partial^2 w}{\partial x\,\partial y}\right)$$

Therefore, it has now been shown that all the natural boundary conditions (eqs. (14), (15), and (17)) and the differential equations of equilibrium (eqs. (11a), (11b), and (11c)) follow from the condition that the first variation of the potential energy of the plate must vanish for all admissible variations in the displacements u, v, and w.

APPENDIX B

ELASTIC SOLUTION

The elastic postbuckling behavior of the two-element plate can be obtained analytically by applying the Rayleigh-Ritz method to the elastic counterpart of the variational problem formulated in the present paper.

The strain energy of stretching and bending of the plate is given by equation (19) except that it is now understood that the relationships between the components of stress and strain are equations (1a) with the local modulus E_s replaced by Young's modulus E. Substitution of these elastic stress-strain relations into equation (18) and integration to the final strain state yield

$$U = \frac{2}{3} Et_f \int_{-b/2}^{b/2} \int_{-b/2}^{b/2} \left[\left(\epsilon_{x_t}^2 + \epsilon_{y_t}^2 + \epsilon_{x_t}\epsilon_{y_t} + \frac{\gamma_{xy_t}^2}{4} \right) + \left(\epsilon_{x_b}^2 + \epsilon_{y_b}^2 + \epsilon_{x_b}\epsilon_{y_b} + \frac{\gamma_{xy_b}^2}{4} \right) \right] dx\, dy \tag{B1}$$

Since the displacements u, v, and w can be related to the strains through the large-deflection strain-displacement relations (6), the strain energy can be written as a function of the unit shortening e and the undetermined coefficients appearing in the displacement expressions (21), (22), and (23). As mentioned earlier, both the plastic and the elastic solutions of the present paper are limited to the determination of only six of the unknown coefficients appearing in the displacement functions. That is, the displacements are assumed to be

$$\left.\begin{aligned} u &= -ex + b\left(u_{10} + u_{11} \cos \frac{2\pi y}{b}\right) \sin \frac{2\pi x}{b} \\ v &= fy + b\left(v_{01} + v_{11} \cos \frac{2\pi x}{b}\right) \sin \frac{2\pi y}{b} \\ w &= bw_{11} \cos \frac{\pi x}{b} \cos \frac{\pi y}{b} \end{aligned}\right\} \tag{B2}$$

where e is the applied unit shortening and the remaining coefficients are to be determined by application of the Rayleigh-Ritz method. The assumed expression for w is exact at initial buckling for a square plate and is assumed to be reasonably accurate in the early postbuckling range.

Through the use of relations (6) and (B2) in equation (B1), the strain-energy density can be integrated over the stress-carrying area of the plate to give

$$U = \frac{4}{3} Et_f b^2 \left\{ e^2 - ef + f^2 + \frac{3}{8}\pi^2(-e + f) + \frac{1}{2}\left[(2\pi u_{10})^2 + (2\pi v_{01})^2\right] - \right.$$
$$\frac{\pi^2}{16}(2\pi u_{10} + 2\pi v_{01}) w_{11}^2 + \frac{5}{16}\left[(2\pi u_{11})^2 + (2\pi v_{11})^2\right] -$$
$$\left. \frac{\pi^2}{8}(2\pi u_{11} + 2\pi v_{11}) w_{11}^2 + \frac{3}{8}(2\pi u_{11})(2\pi v_{11}) + \frac{5}{64}\pi^4 w_{11}^4 + \frac{\pi^2}{4}\left(\frac{\pi h}{b}\right)^2 w_{11}^2 \right\} \tag{B3}$$

The conditions for obtaining the values of the coefficients that minimize the strain energy for a given value of the unit shortening are

$$\frac{\partial U}{\partial f} = \frac{\partial U}{\partial u_{10}} = \frac{\partial U}{\partial v_{01}} = \frac{\partial U}{\partial u_{11}} = \frac{\partial U}{\partial v_{11}} = \frac{\partial U}{\partial w_{11}} = 0$$

After the operations indicated by the minimizing conditions are performed, the following six simultaneous equations are obtained for evaluating the six unknown coefficients:

$$\left.\begin{aligned}
&-\frac{e}{2} + f + \frac{3}{16}\pi^2 w_{11}^2 = 0 \\
&2(2\pi u_{10}) - \frac{\pi^2}{8} w_{11}^2 = 0 \\
&2(2\pi v_{01}) - \frac{\pi^2}{8} w_{11}^2 = 0 \\
&\frac{5}{4}(2\pi u_{11}) + \frac{3}{4}(2\pi v_{11}) - \frac{\pi^2}{4} w_{11}^2 = 0 \\
&\frac{3}{4}(2\pi u_{11}) + \frac{5}{4}(2\pi v_{11}) - \frac{\pi^2}{4} w_{11}^2 = 0 \\
&w_{11}\left[\frac{3}{2}(-e + f) - \frac{1}{2}\left(\frac{2\pi u_{10} + 2\pi v_{01}}{2} + 2\pi u_{11} + 2\pi v_{11}\right) + \right. \\
&\qquad \left. \left(\frac{\pi h}{b}\right)^2 + \frac{5}{8}\pi^2 w_{11}^2\right] = 0
\end{aligned}\right\} \tag{B4}$$

Solution of the first five of equations (B4) yields

$$\left.\begin{aligned} f &= \frac{e}{2} - \frac{3}{16}\pi^2 w_{11}^2 \\ 2\pi u_{10} &= 2\pi v_{01} = \frac{\pi^2}{16} w_{11}^2 \\ 2\pi u_{11} &= 2\pi v_{11} = \frac{\pi^2}{8} w_{11}^2 \end{aligned}\right\} \tag{B5}$$

Substitution of relations (B5) into the last of equations (B4) gives

$$w_{11}\left[-e + \frac{4}{3}\left(\frac{\pi h}{b}\right)^2 + \frac{\pi^2}{4} w_{11}^2\right] = 0 \tag{B6}$$

In general, $w_{11} \neq 0$; hence,

$$-e + \frac{4}{3}\left(\frac{\pi h}{b}\right)^2 + \frac{\pi^2}{4} w_{11}^2 = 0 \tag{B7}$$

Now, when w_{11} vanishes, the criterion for initial buckling is established; that is, the critical strain or shortening becomes

$$e_{cr} = \frac{4}{3}\left(\frac{\pi h}{b}\right)^2 \tag{B8}$$

and, in turn, the compressive buckling stress is simply

$$\sigma_{cr} = \frac{4}{3} E\left(\frac{\pi h}{b}\right)^2$$

As a consequence of equation (B8), equation (B7) yields the nondimensional center deflection of the plate as

$$w_{11}^2 = \frac{4}{\pi^2}\left(e - e_{cr}\right) \tag{B9}$$

and, hence, the six coefficients are completely determined for any value of the plate unit shortening and cross-section geometry.

By virtue of the results (B5) and (B9), the displacement expressions (B2) can be substituted into the stress-displacement relations (7) (with $E_s = E$) to obtain the stresses present in the faces of the two-element plate. In terms of average stress (see relations (10)), the results of this substitution yield

$$\left.\begin{aligned}
\frac{\sigma_x}{\sigma_{cr}} &= -\frac{1}{2}\left[\left(\frac{e}{e_{cr}} + 1\right) - \left(\frac{e}{e_{cr}} - 1\right)\cos\frac{2\pi y}{b}\right] \\
\frac{\sigma_y}{\sigma_{cr}} &= \frac{1}{2}\left(\frac{e}{e_{cr}} - 1\right)\cos\frac{2\pi x}{b} \\
\frac{\tau_{xy}}{\sigma_{cr}} &= 0
\end{aligned}\right\} \tag{B10}$$

It should be mentioned that, although the stress expressions (B10) were obtained on the basis of two-element-plate geometry and a Poisson's ratio of 1/2, a rederivation for the case of a solid plate, with an arbitrary Poisson's ratio, yields the identical results for the stresses.

It is of interest to note that the approximate elastic solution (eqs. (B10)) for the stresses turns out to satisfy the equilibrium equations (11a) and (11b) exactly at each point of the plate; the third equilibrium equation (eq. (11c)) is, of course, not satisfied. A measure of the accuracy of the approximate elastic solution is afforded by figure 8, which compares the approximate relationship found between σ_{av}/σ_{cr} and e/e_{cr} with the exact relationship found by Levy.

Equations (B5) and (B9) determined in this appendix are used as initial values in the minimizing procedure for determining the solution to the plastic-plate problem. (See appendix C.)

APPENDIX C

PLASTIC SOLUTION

The variational problem is conveniently formulated in nondimensional terms as follows: Let $\xi = 2x/b$ and $\eta = 2y/b$; and let

$$G\left(\epsilon_{eff}\right) = \frac{1}{E}\int_0^{\epsilon_{eff}} \sigma_{eff}\, d\epsilon_{eff}$$

Since the four quadrants of the plate behave identically, the energy integral (20) may be modified into the nondimensional form

$$F = \frac{4U}{Et_f b^2} = \int_0^1 \int_0^1 \left[G\left(\epsilon_{eff_t}\right) + G\left(\epsilon_{eff_b}\right)\right] d\xi\, d\eta \tag{C1}$$

Here ϵ_{eff} is given by equations (8) in terms of ϵ_x, ϵ_y, and γ_{xy}, which in turn are found from equations (6), (21), (22), and (23) to depend only on the spatial coordinates ξ and η, on the applied unit shortening e, and on the unknown nondimensional parameters

$$\left.\begin{array}{ll} 2\pi u_{10} & 2\pi v_{01} \\ 2\pi u_{11} & 2\pi v_{11} \\ f & \frac{\pi h}{b} w_{11} \end{array}\right\} \tag{C2}$$

The ratio $\frac{\pi h}{b}$ fixes the magnitude of the critical shortening e_{cr} and hence specifies the plate geometry. The set of six nondimensional parameters (C2) are to be so determined as to minimize F for given values of $\frac{\pi h}{b}$ and e.

Since analytical minimization of F is not feasible when nonlinear stress-strain relations are involved, recourse is had to a numerical minimization process in conjunction with the use of a high-speed computing machine (SEAC). The minimization process was effected by means of, essentially, the so-called "method of steepest descents." (See, for example, refs. 20 and 21.)

The basic idea of the procedure may be described in general terms as follows: Consider a function $F(x_1, x_2, \ldots x_n)$. The set of n independent parameters may be conveniently denoted by the n-component vector x_i $(i = 1, 2, 3, \ldots n)$. The value of x_i that minimizes F is sought. An initial trial vector $x_i^{(0)}$ is assumed, and the gradient of F, that is, $\frac{\partial F}{\partial x_i}$, is calculated at $x_i^{(0)}$. The direction $-\frac{\partial F}{\partial x_i}$ is then the direction of steepest descent of the function F; the function $F\left[x_i^{(0)} - \delta\frac{\partial F}{\partial x_i}\right]$ is then evaluated for various positive values of δ in an effort to find the value $\bar{\delta}$ that minimizes $F\left[x_i^{(0)} - \delta\frac{\partial F}{\partial x_i}\right]$. When this value of $\bar{\delta}$ is found (presumably, approximately), a new direction of steepest descent is determined by evaluation of the gradient of F at the point $x_i^{(1)} = x_i^{(0)} - \bar{\delta}\frac{\partial F}{\partial x_i}\left[x_i^{(0)}\right]$. The process is continued until satisfactory convergence is obtained to the lowest possible value of F. In the present problem, the six parameters in the set (eq. (C2)) play the role of the components of the vector x_i.

In the application of the method of steepest descents, the basic procedure outlined above was modified in certain respects. First of all, each evaluation of F was performed approximately by means of numerical integration. Each face of the quarter plate was divided into a grid of 100 squares, the integrand in equation (C1) was computed at each grid point, and the integral was evaluated by applying Simpson's rule twice - once for the integration in the ξ-direction and once for the η-direction. For this calculation, the function G was represented, piecewise, by polynomials determined from the stress-strain relationship of figure 2.

The evaluation of the gradient of F was performed on the basis of a finite-difference approximation to each of the six partial derivatives required. Thus, the determination of the six components of $\frac{\partial F}{\partial x_i}$ necessitated seven evaluations of F - one at the particular set of starting values of the independent variables and one each for a small increment in one of the six variables.

In any given cycle, the value of $\bar{\delta}$ in the starting point $x_i - \bar{\delta}\frac{\partial F}{\partial x_i}$ of the succeeding cycle was found by passing a parabola through the three points $F(0)$, $F(\delta)$, and $F(2\delta)$ given by the values of F at x_i, $x_i - \delta\frac{\partial F}{\partial x_i}$, and $x_i - 2\delta\frac{\partial F}{\partial x_i}$. Here δ was chosen to be of some convenient magnitude, preferably of the order expected for $\bar{\delta}$.

It is pointed out in reference 20 that, in practical application, the method of steepest descents tends to furnish successive approximations to the minimizing vector that zigzag toward the true minimum rather than approach it in a smooth fashion. Consequently, the following procedure was introduced in an attempt to speed up convergence: After two successive cycles of minimization in the direction of the negative gradient, a third cycle of a different nature was inserted. In this extra cycle, minimization was performed not in the direction of the negative gradient, but rather in the direction determined by the differences between the last-obtained approximations to the unknowns and the approximations of two cycles before. Thus, a round of three successive approximations to the minimum vector proceeded as follows:

(1) Given x_i^n; find $\frac{\Delta F}{\Delta x_i}\left(x_i^n\right)$; minimize $F\left[x_i^n - \delta\frac{\Delta F}{\Delta x_i}\left(x_i^n\right)\right]$ to find $\bar{\delta}_n$; obtain $x_i^{n+1} = x_i^n - \bar{\delta}_n \frac{\Delta F}{\Delta x_i}\left(x_i^n\right)$.

(2) Repeat step (1), starting with x_i^{n+1}; this procedure gives

$$x_i^{n+2} = x_i^{n+1} - \bar{\delta}_{n+1} \frac{\Delta F}{\Delta x_i}\left(x_i^{n+1}\right).$$

(3) Let $S_i = x_i^n - x_i^{n+2}$; minimize $F\left(x_i^{n+2} - \delta S_i\right)$ to obtain $\bar{\delta}_{n+2}$; then, $x_i^{n+3} = x_i^{n+2} - \bar{\delta}_{n+2} S_i$.

(4) Repeat steps (1), (2), and (3) as many times as are necessary to obtain satisfactory convergence to the minimizing value of x_i.

It may be remarked that in practice the quantities $\frac{\Delta F}{\Delta x_i}$ and S_i were normalized; that is, each component of a set $\frac{\Delta F}{\Delta x_i}$ or S_i was divided by the absolute value of the largest component.

It is clear that a tremendous amount of numerical calculation is involved in the application of this procedure to the present problem; only very high computing speeds make such a procedure feasible.

For each value of $\frac{\pi h}{b}$ and e, the initial values assumed in the iteration process were taken from the elastic solution of appendix B. Convergence to the minimum energy level was considered satisfactory if several successive cycles yielded the same value of energy to within

four significant figures. About thirteen cycles of iteration, involving approximately 35 minutes of computing time for the SEAC, were generally required for convergence. In several instances, particularly at the highest unit shortenings, convergence was found to be impracticably slow; in these few cases, the minimum energy level was estimated by evaluating it for values of the displacement coefficients extrapolated from curves such as are shown in figures 3 and 4. The final plots for energy against unit shortening obtained for the four plates are shown in figure 6.

It is of interest that the total difference in energy between the first and last cycles of iteration for any one case was always very small (of the order of 1 percent). Consequently, as far as the energy is concerned, a fair estimate could be found on the basis of the elastic displacement coefficients. However, as is discussed in the body of the present paper, a reasonably accurate estimate of the stress distribution requires application of the minimization process.

REFERENCES

1. Von Kármán, Th.: Festigkeitsprobleme in Maschinenbau. Vol. IV, pt. 4 of Encyk. der Math. Wiss., 1910, art. 27, p. 349.

2. Von Kármán, Theodor, Sechler, Ernest E., and Donnell, L. H.: The Strength of Thin Plates in Compression. A.S.M.E. Trans., APM-54-5, vol. 54, no. 2, Jan. 30, 1932, pp. 53-57.

3. Cox, H. L.: The Buckling of Thin Plates in Compression. R. & M. No. 1554, British A.R.C., 1933.

4. Timoshenko, S.: Theory of Elastic Stability. McGraw-Hill Book Co., Inc., 1936, pp. 287-418.

5. Marguerre, K., and Trefftz, E.: Über die Tragfähigkeit eines längsbelasteten Plattenstreifens nach Überschreiten der Beullast. Z.f.a.M.M., Bd. 17, Heft 2, Apr. 1937, pp. 85-100.

6. Marguerre, Karl: Apparent Width of the Plate in Compression. NACA TM 833, 1937.

7. Kromm, A., and Marguerre, K.: Behavior of a Plate Strip Under Shear and Compressive Stresses Beyond the Buckling Limit. NACA TM 870, 1938.

8. Levy, Samuel: Bending of Rectangular Plates With Large Deflections. NACA Rep. 737, 1942.

9. Koiter, W. T.: De meedragende breedte bij groote overschrijding der knikspanning voor verschillende inklemming der plaatranden. (The Effective Width of Infinitely Long, Flat Rectangular Plates Under Various Conditions of Edge Restraint.) Rep. S.287, Nationaal Luchtvaartlaboratorium, Amsterdam, Dec. 1943.

10. Hu, Pai C., Lundquist, Eugene E., and Batdorf, S. B.: Effect of Small Deviations From Flatness on Effective Width and Buckling of Plates in Compression. NACA TN 1124, 1946.

11. Coan, J. M.: Large-Deflection Theory for Plates With Small Initial Curvature Loaded in Edge Compression. Jour. Appl. Mech., vol. 18, no. 2, June 1951, pp. 143-151.

12. Stowell, Elbridge Z.: A Unified Theory of Plastic Buckling of Columns and Plates. NACA Rep. 898, 1948. (Supersedes NACA TN 1556.)

13. Bijlaard, P. P.: Theory and Tests on the Plastic Stability of Plates and Shells. Jour. Aero. Sci., vol. 16, no. 9, Sept. 1949, pp. 529-541.

14. Greenberg, H. J.: On the Variational Principles of Plasticity. Rep. A11-S4 (Contract N7onr-358, T.O.1, NR-041-032), Graduate Div. Appl. Math., Brown Univ., Mar. 1949.

15. Kauffman, William M., and Shinbrot, Marvin: A Method for Differentiation of Experimental Data. Jour. Aero. Sci. (Readers' Forum), vol. 20, no. 6, June 1953, pp. 428-430.

16. Schuman, Louis, and Back, Goldie: Strength of Rectangular Flat Plates Under Edge Compression. NACA Rep. 356, 1930.

17. Needham, Robert A.: The Ultimate Strength of Aluminum-Alloy Formed Structural Shapes in Compression. Jour. Aero. Sci., vol. 21, no. 4, Apr. 1954, pp. 217-229.

18. Botman, M.: De experimentele bepaling van de meedragende breedte van vlakke platen in het elastische en het plastische gebied (deel II). (The Experimental Determination of the Effective Width of Flat Plates in the Elastic and Plastic Range (part II).) Rep. S.438, Nationaal Luchtvaartlaboratorium, Amsterdam, Jan. 1954.

19. Besseling, J. F.: De experimentele bepaling van de meedragende breedte van vlakke platen in het elastische en het plastische gebied. (The Experimental Determination of the Effective Width of Flat Plates in the Elastic and Plastic Range.) Rep. S.414, Nationaal Luchtvaartlaboratorium, Amsterdam, Feb. 1953.

20. Hartree, Douglas R.: Some Unsolved Problems in Numerical Analysis. Problems for the Numerical Analysis of the Future, Appl. Math. Series 15, National Bur. Standards, June 29, 1951, pp. 1-9.

21. Curry, Haskell B.: The Method of Steepest Descent for Non-Linear Minimization Problems. Quarterly Appl. Math., vol. II, no. 3, Oct. 1944, pp. 258-261.

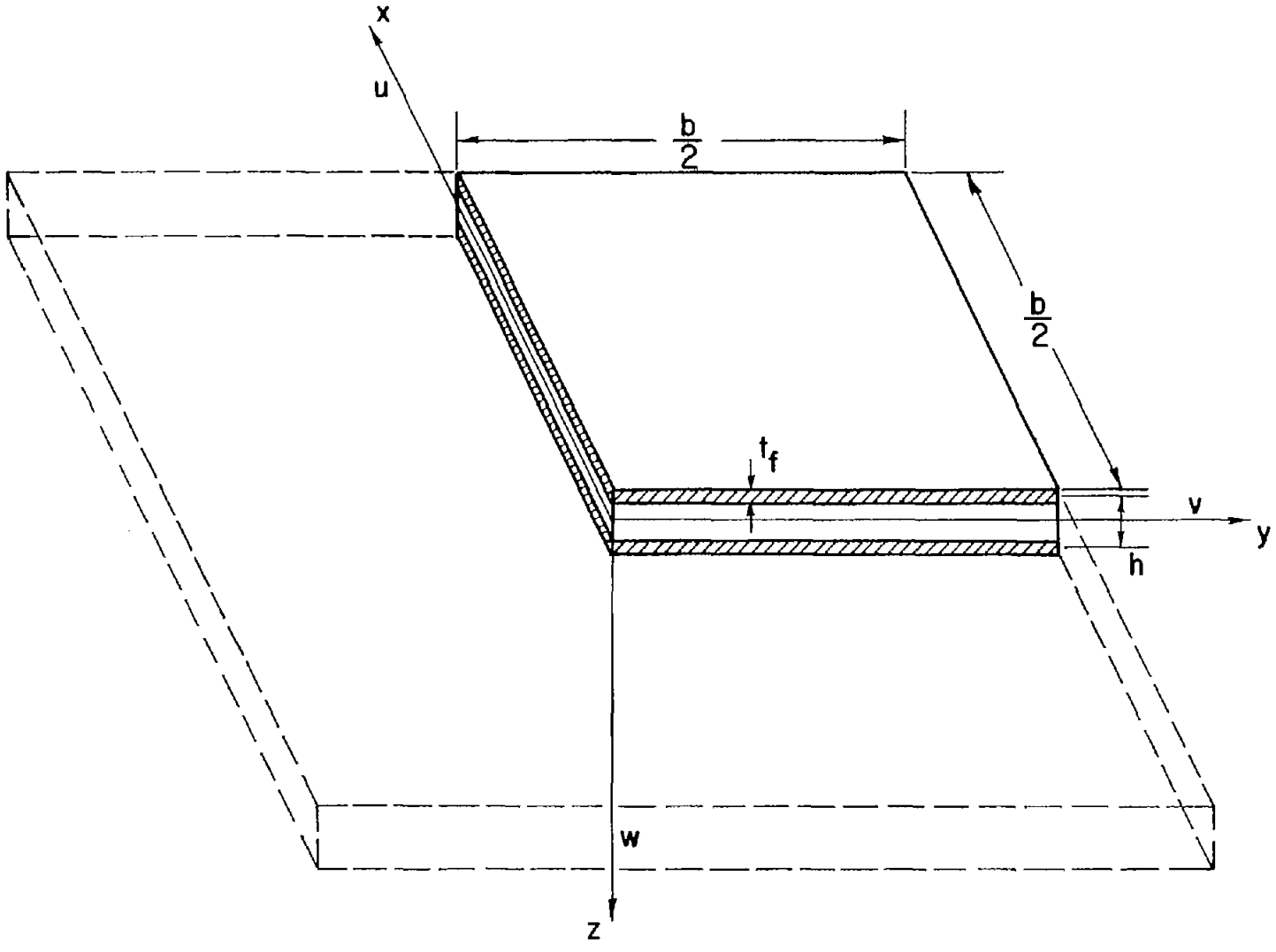

Figure 1.- Plate geometry and coordinate system.

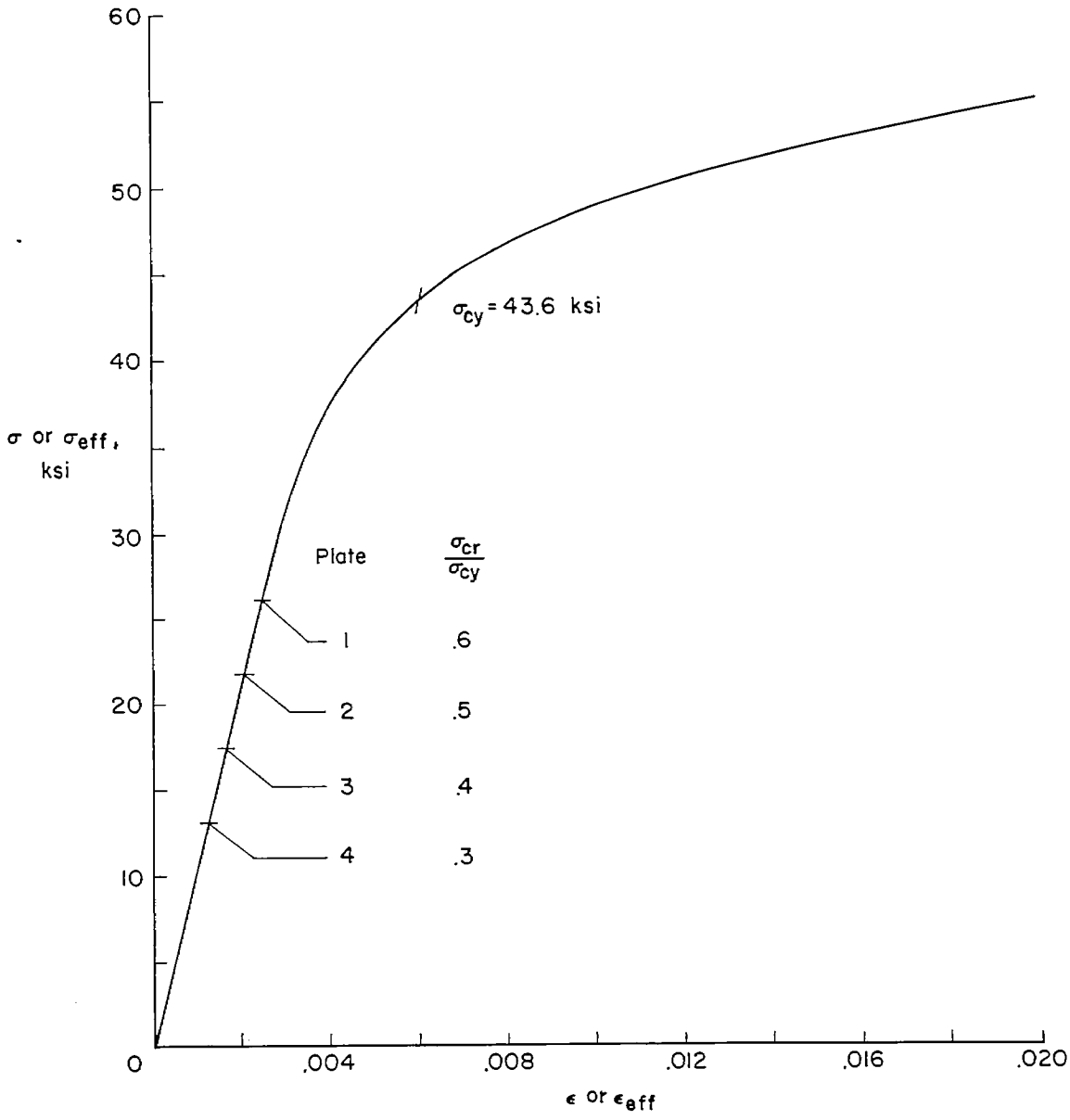

Figure 2.- Compressive stress-strain curve and initial buckling stresses for 24S-T aluminum-alloy plates analyzed.

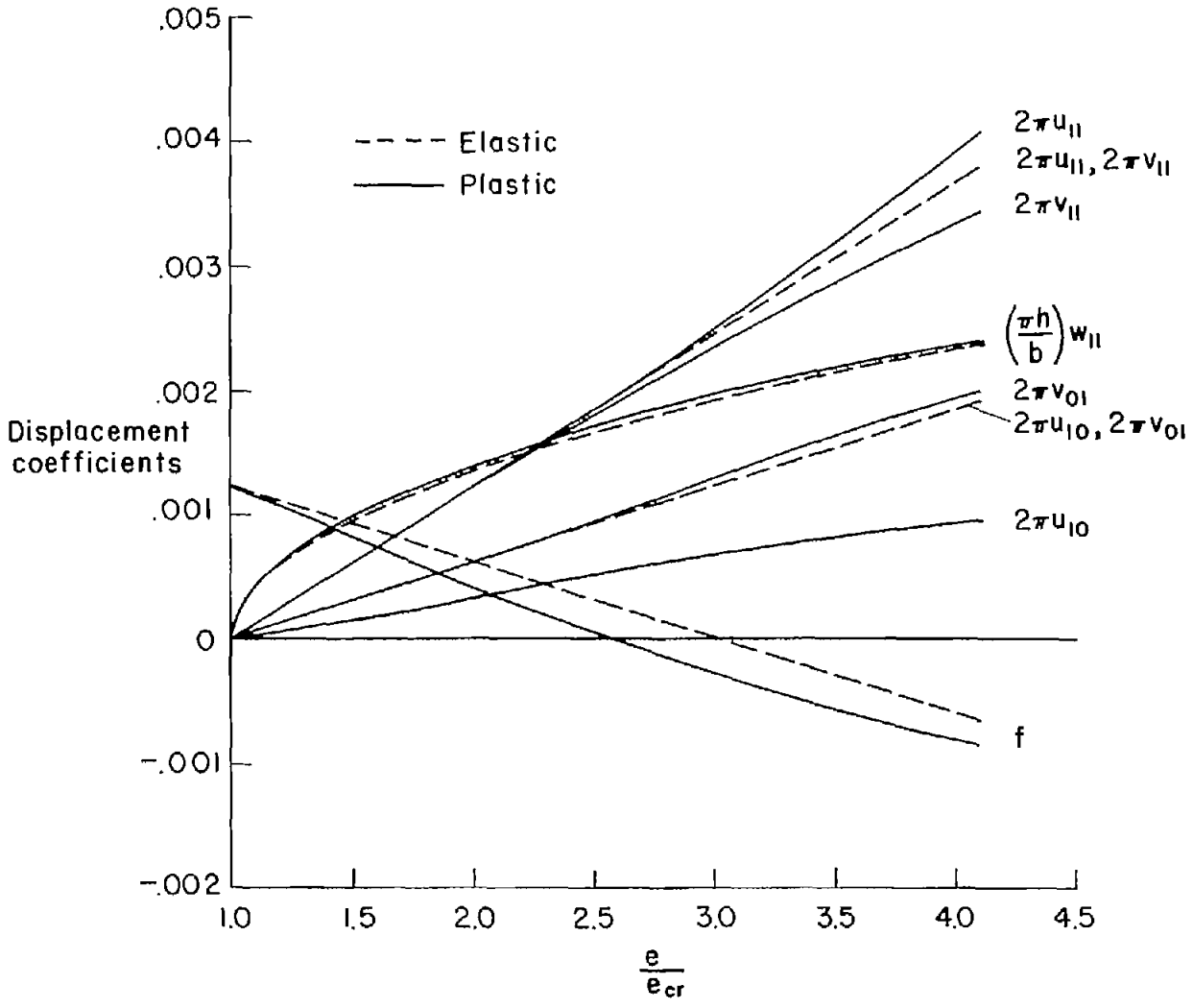

Figure 3.- Variation of displacement-coefficient values with unit shortening for plate 1.

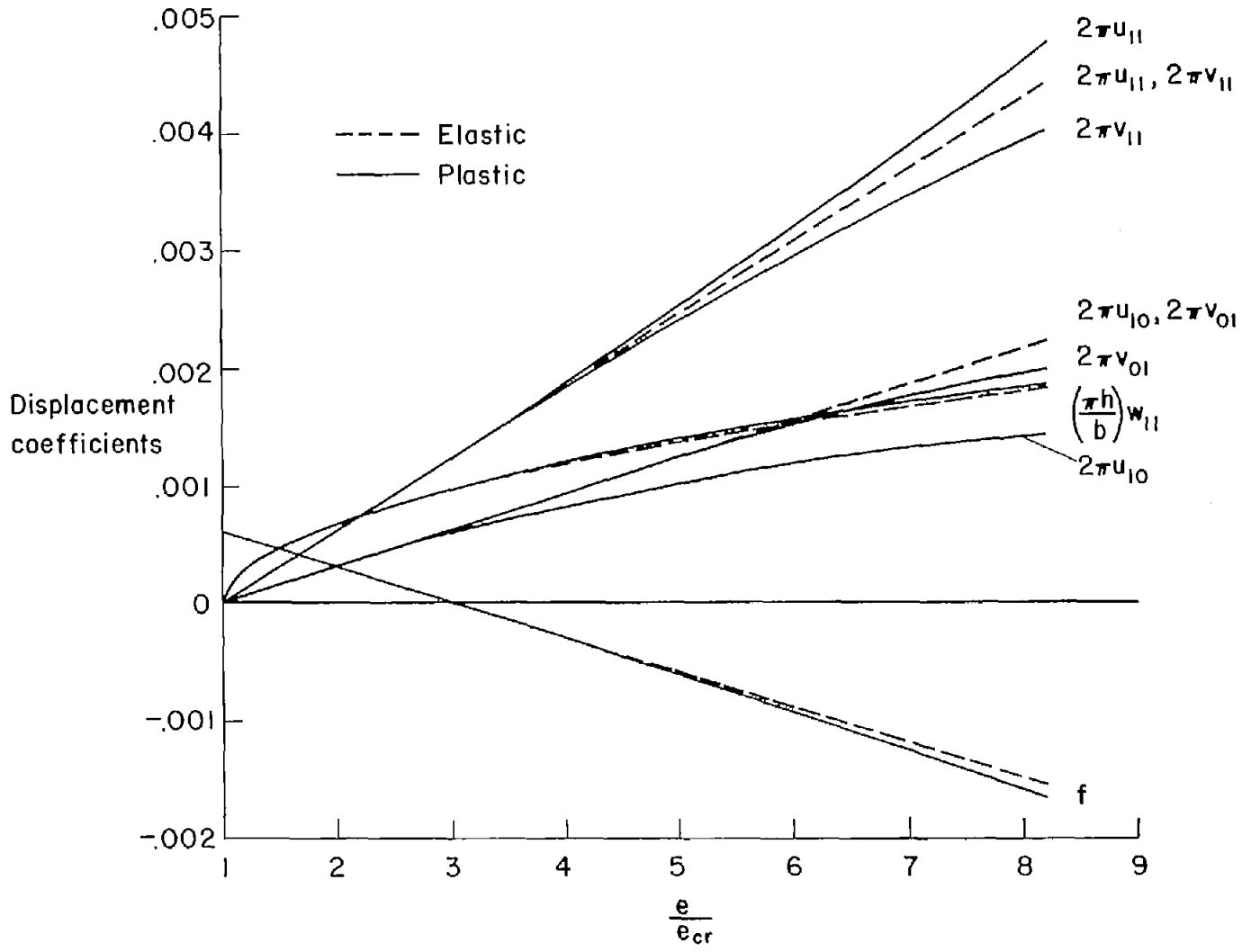

Figure 4.- Variation of displacement-coefficient values with unit shortening for plate 4.

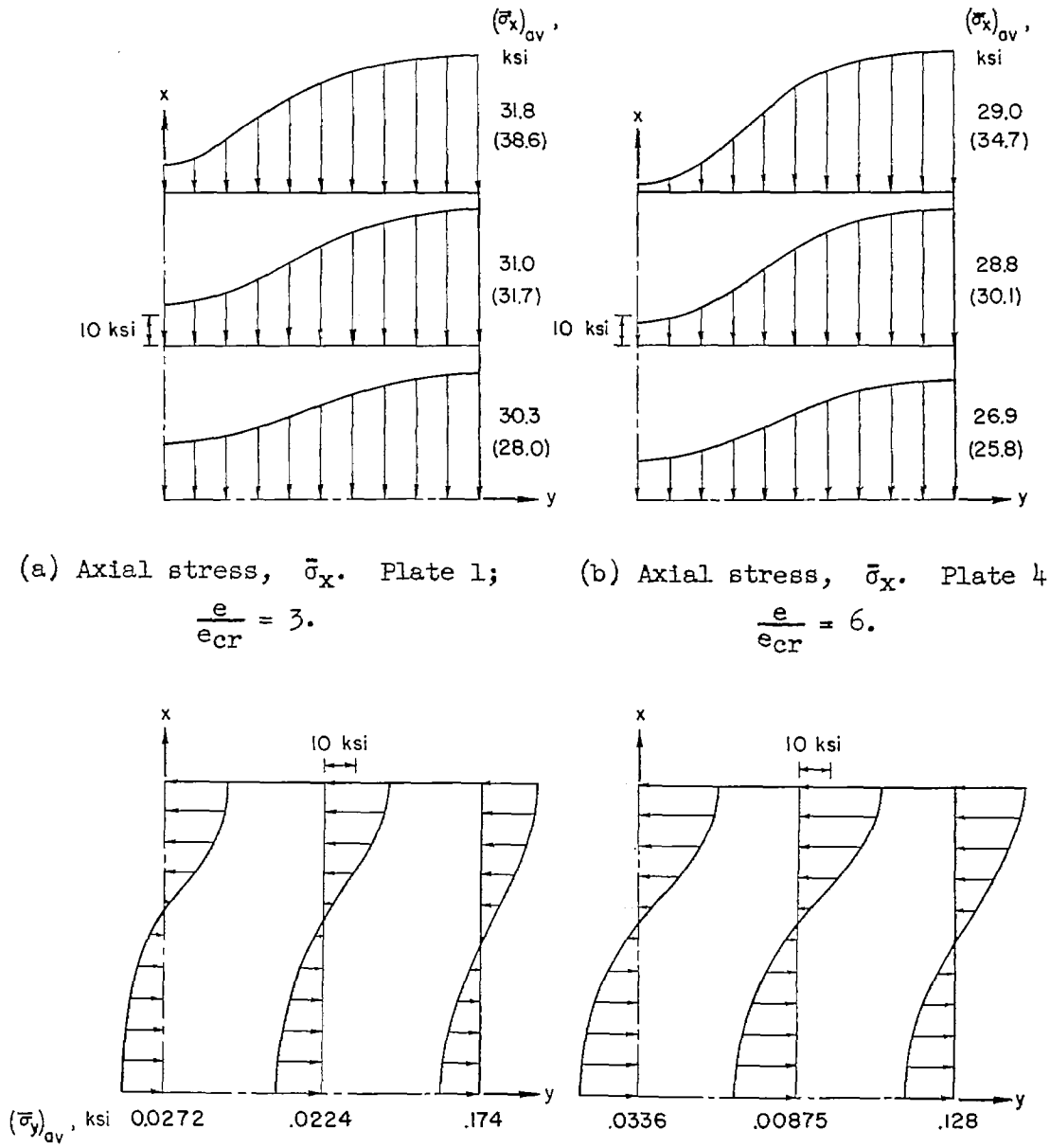

(a) Axial stress, $\bar{\sigma}_x$. Plate 1; $\frac{e}{e_{cr}} = 3.$

(b) Axial stress, $\bar{\sigma}_x$. Plate 4; $\frac{e}{e_{cr}} = 6.$

(c) Lateral stress, $\bar{\sigma}_y$. Plate 1; $\frac{e}{e_{cr}} = 3.$

(d) Lateral stress, $\bar{\sigma}_y$. Plate 4; $\frac{e}{e_{cr}} = 6.$

Figure 5.- Axial and lateral stress distributions for first quadrant of plates 1 and 4. (Values in parentheses refer to average stress based on elastic displacements.)

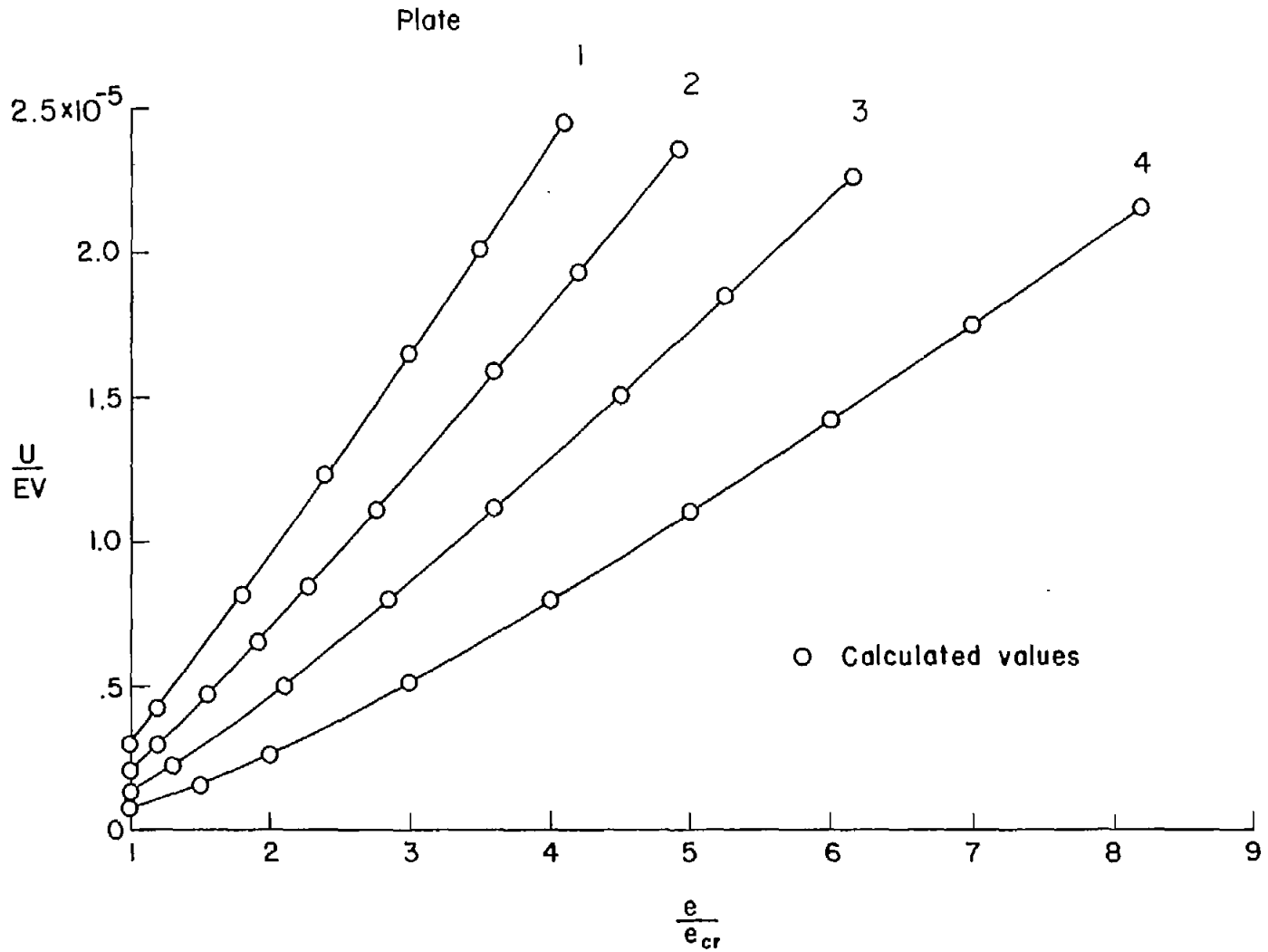

Figure 6.- Relationship between strain energy and applied unit shortening for plates analyzed.

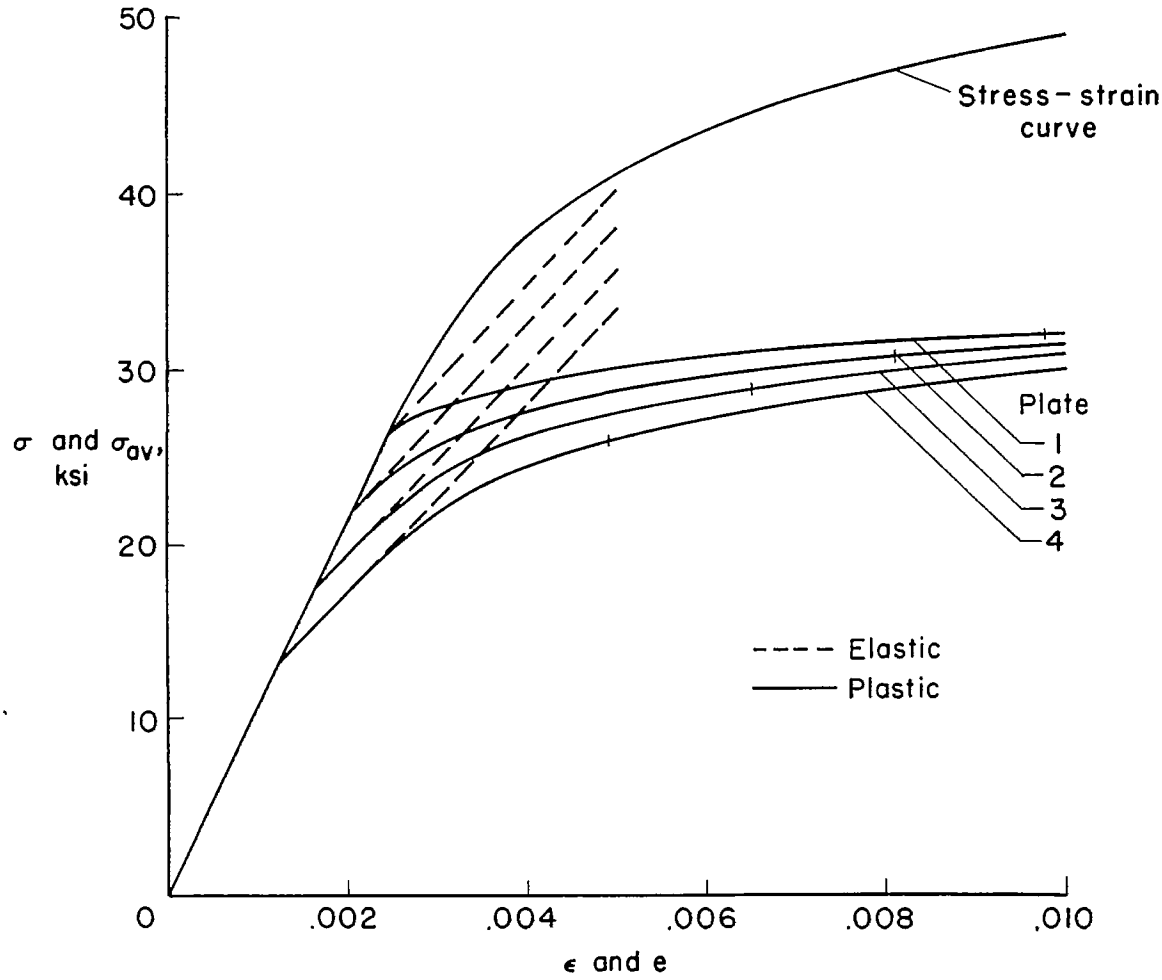

Figure 7.- Variation of average compressive stress with unit shortening (unadjusted).

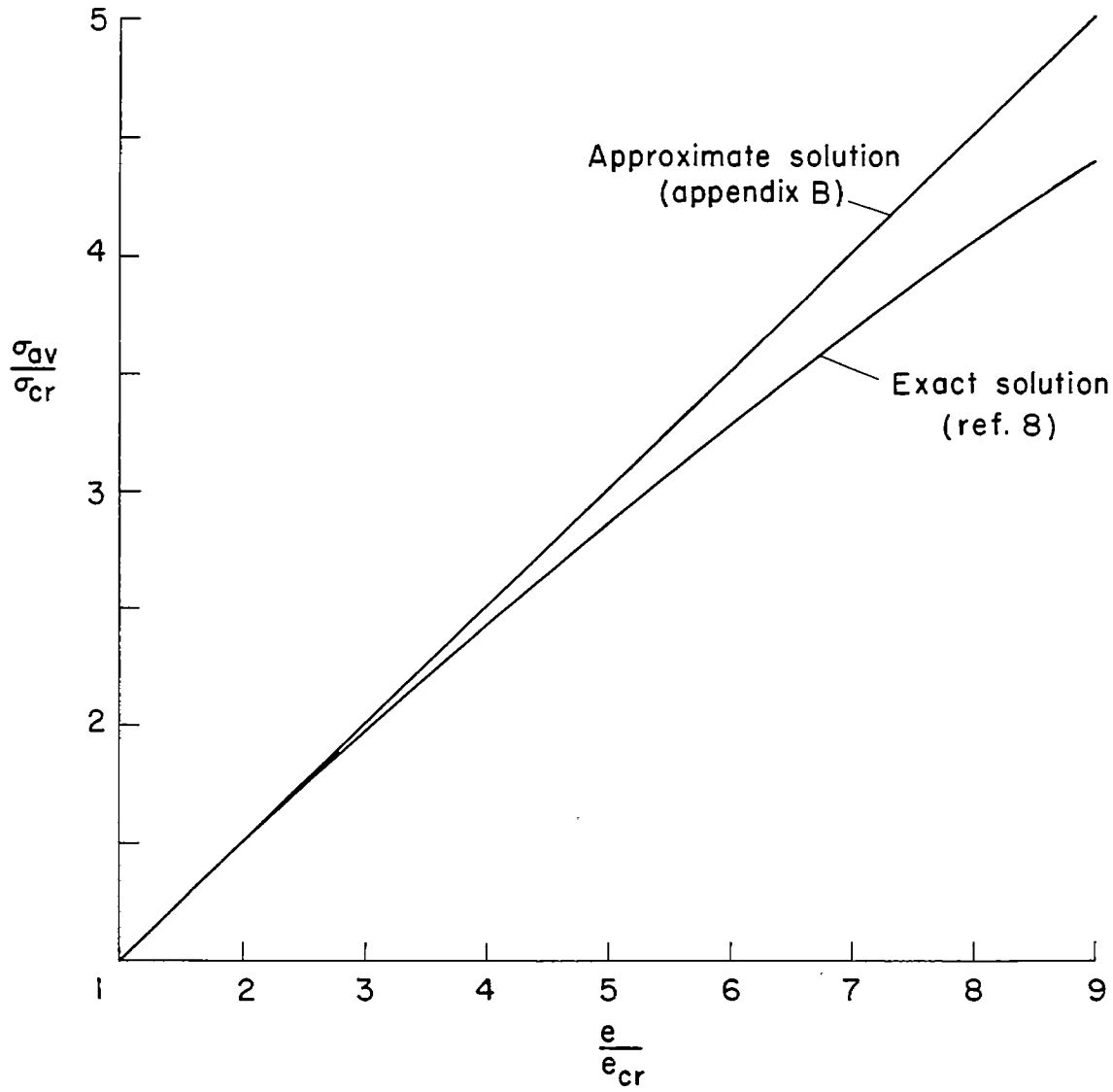

Figure 8.- Comparison of approximate and exact elastic solutions for the average compressive stress carried by a buckled plate.

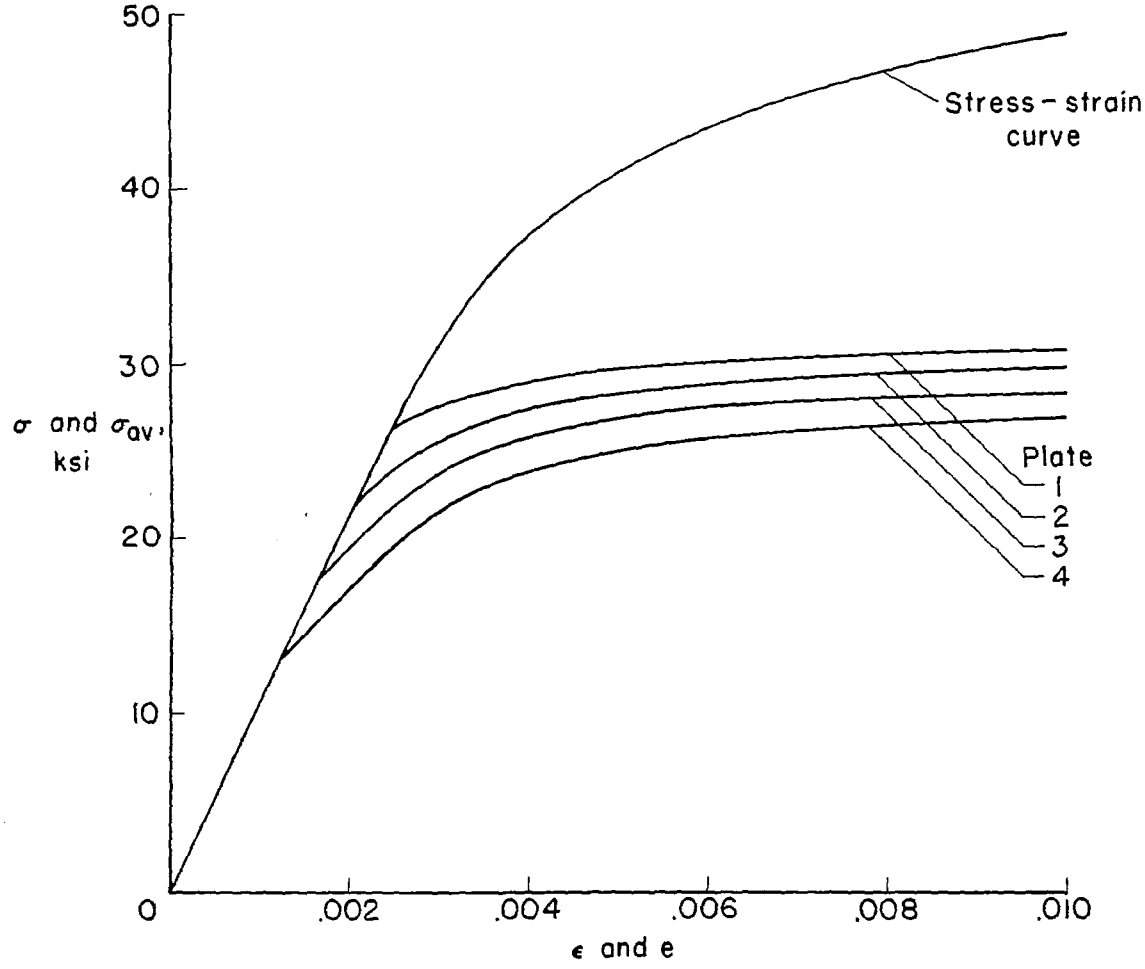

Figure 9.- Variation of average compressive stress with unit shortening (adjusted).

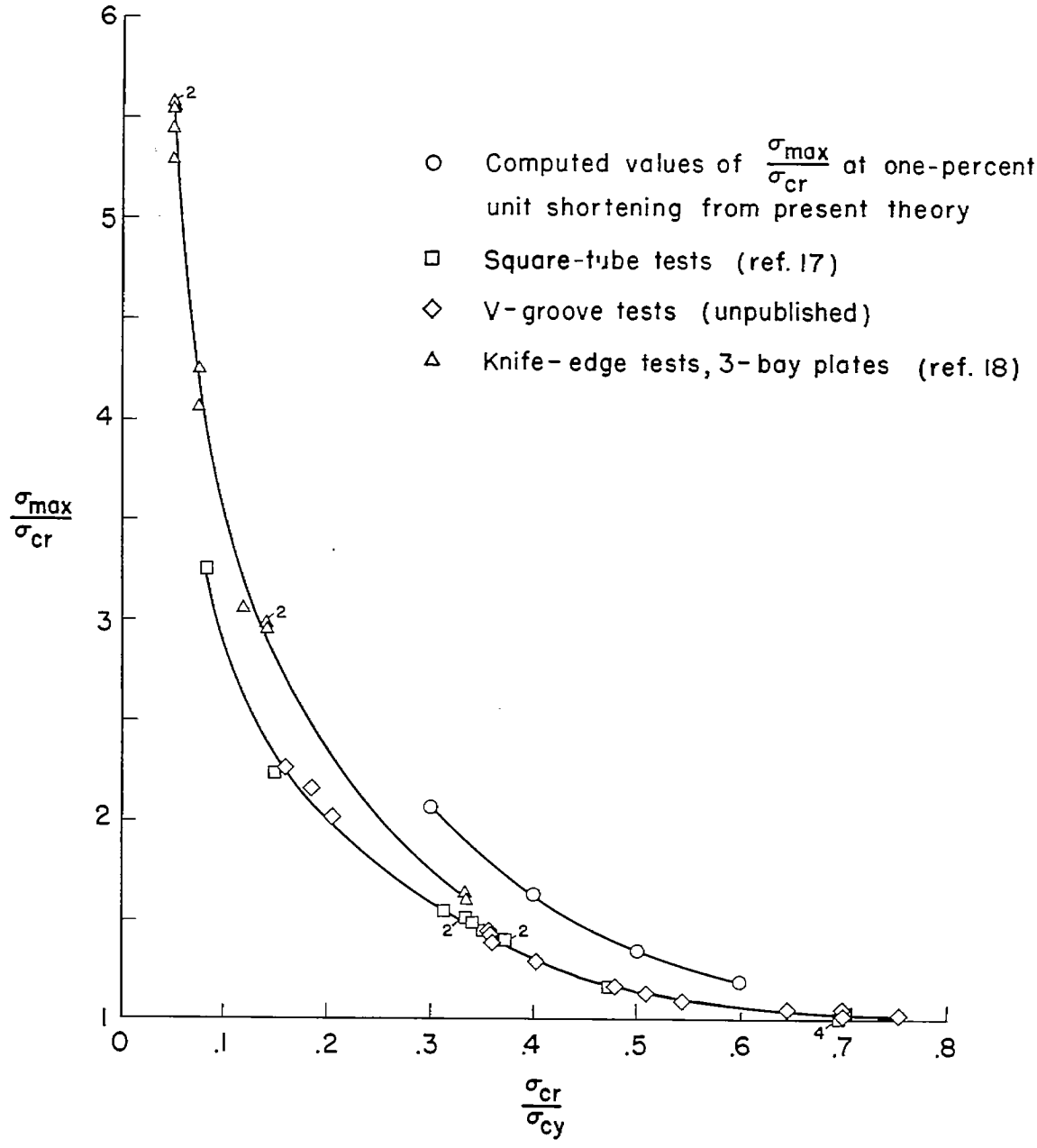

Figure 10.- Comparison of experimental and calculated results for compressive strength of flat plates.

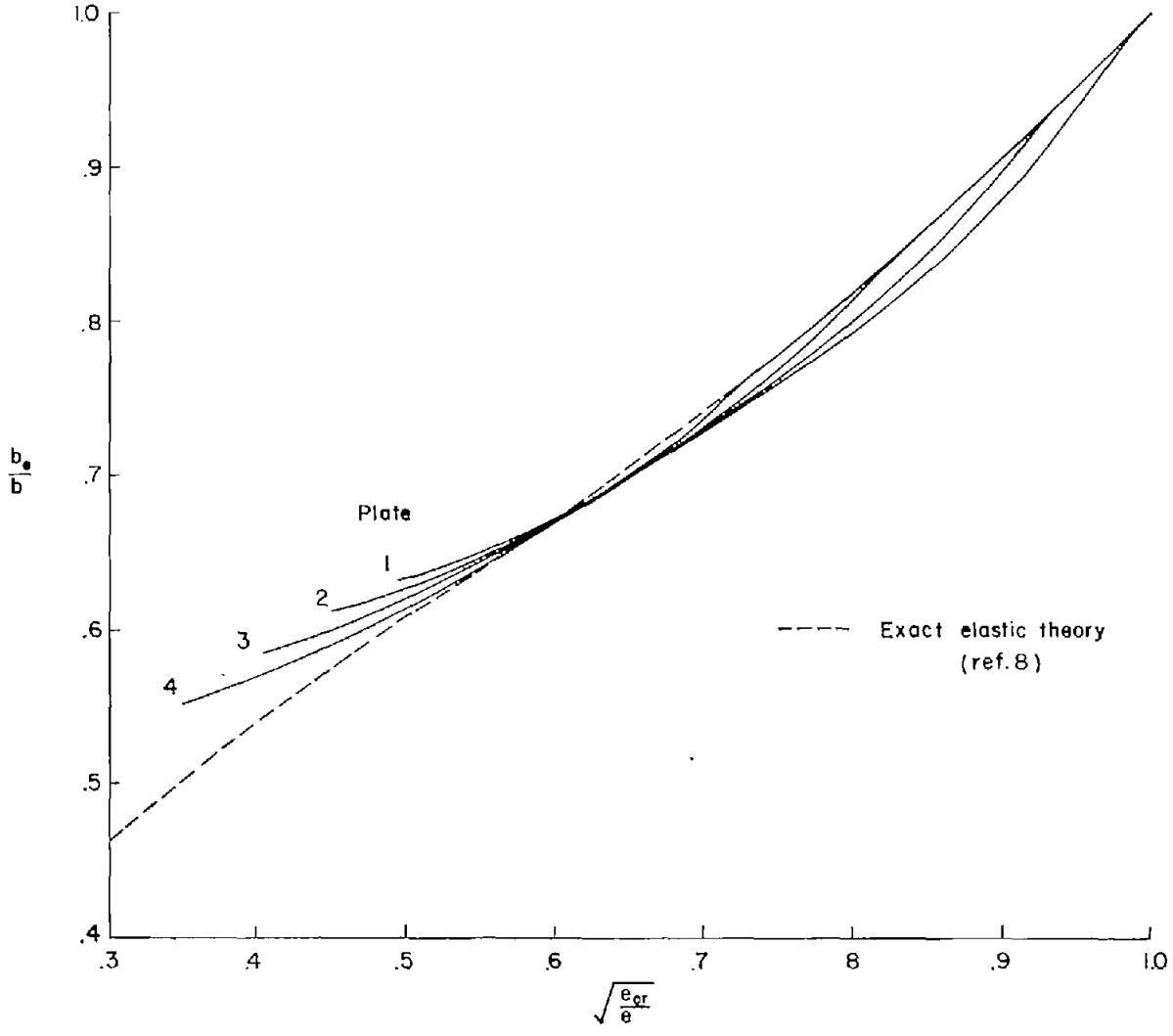

Figure 11.- Effective widths obtained from present solution compared with results of Levy's exact elastic analysis (ref. 8).

NACA-Langley - 2-28-55 - 1000